NETWORK DESIGN AND OPTIMIZATION FOR DEFORMATION MONITORING ON TUZLA FAULT-IZMIR AND ITS VICINITY

by

Kerem Halicioğlu

B.S., İstanbul Technical University, 2003

Submitted to the Kandilli Observatory and
Earthquake Research Institute in partial fulfillment of
the requirements for the degree of
Master of Science

Graduate Program in Geodesy

Boğaziçi University

2007

NETWORK DESIGN AND OPTIMIZATION FOR DEFORMATION MONITORING ON TUZLA FAULT-IZMIR AND ITS VICINITY

APPROVED BY:

Assoc. Prof. Haluk Özener ……..

Prof. Onur Gürkan ……..

Prof. Rasim Deniz ……..

DATE OF APPROVAL:

ACKNOWLEDGEMENTS

This study becomes realized with many valuable contributions. Firstly I would like to thank to my supervisor, Assoc. Prof. Dr. Haluk Özener for his great support, guidance and encouragement for this study. Moreover, beginning from the constitution of the project, I am very grateful to Dr. Ahmet Ünlütepe for his evaluations and discussions on the study.

I am grateful to Prof. Dr. Onur Gürkan for his advices, and comments.. I thank to lecturer Esen Arpat for his suggestions. I acknowledge Bülent Turgut for his contribution to the reconnaissance to the study area and for his accompany to my processing studies. Moreover, I would like to thank to Asli Garagon Doğru, for her support. I am also thankful to Assistant Professor D.Ugur Şanlı and Dr. Onur Yılmaz. I am very grateful to Ahmet Altın.

I am grateful to Prof. Dr. Gülay Altay, director of the Boğaziçi University Kandilli Observatory and Earthquake Research Institute, for her support.

I want to declare the contribution of Zeynep Özege from Izmir Manucipility of Greater City, Zafer Beydilli from Bank of Provinces and Engin Paşaoğlu from Seferihisar Branch of General Directorate of Land Registry and Cadastre.

I would like to express my sincere to my friend and classmate Özgür Avcı for his endless cooperation. Finally, I am very grateful to my family for their great thrust and support and all my dear friends.

ABSTRACT

NETWORK DESIGN AND OPTIMIZATION FOR DEFORMATION MONITORING ON TUZLA FAULT-IZMIR AND ITS VICINITY

Seismological and geodynamic researches emphasize that the Aegean Region which comprises the Hellenic Arc, Greek mainland and western Turkey is the most seismically active region in western Eurasia. The convergence of Eurasian and African lithospheric plates forces a westward motion on the Anatolian plate relative to the Eurasia.

Western Anatolia is a valuable laboratory for Earth sciences because of its complex geological structure. Izmir as a big metropolitan city in Turkey with a 2.5 million population has a great risk about big earthquakes. Unfortunately, geodynamics studies which were performed in this region are insufficient or cover large areas instead of specific faults.

This study aims to perform a large scale investigation focusing on Tuzla Fault and its vicinity for better understanding of region tectonics. Tuzla Fault forms the lineament trending NE–SW between Menderes Town and Doganbey Cape. Moreover, Tuzla Fault is an important fault in terms of seismic activities and the distance to the highly populated metropolitan city of Izmir. In order to investigate the crustal deformation on Tuzla Fault and Izmir Bay, a geodetic network has been designed and optimizations were performed. This project produced a schedule for crustal deformation monitoring study which includes research on the tectonics of the region, network design and optimization strategies, theory and practice of processing. The study is also open for extension of study area in terms of monitoring different types of fault characteristics.

ÖZET

TUZLA FAYI-İZMİR VE ÇEVRESİNDEKİ DEFORMASYONLARI İZLEME AMAÇLI AĞ TASARIMI VE OPTİMİZASYONU

Sismolojik ve Jeodinamik çalışmalar, Helenik yay, Yunan anakarası ve Türkiye'nin batısı ile sınırlanan Ege Bölgesinin Alp- Himalaya dağ kuşağının en fazla deformasyona uğrayan bölümlerinden biri olduğunu göstermektedir. Afrika ve Avrasya levhalarının hareketleri, Anadolu levhası üzerinde batıya, saat akrebinin tersi yönünde bir hareket eğilimi yaratmıştır. Ege Bölgesi gerek bu karmaşık hareketliliği ile gerekse bölgede gelişmiş normal ve yanal atımlı faylar nedeniyle yerbilimciler için ilgi çekici bir çalışma alanı olarak öne çıkmıştır. Bölgede bulunan 2.5 milyon nüfuslu (2000 Nüfus sayımı) İzmir şehri de bölgede gerçekleştirilen çalışmaların önemini arttırmıştır. Çalışma gerçekleştirilen alan bu nedenle sismik riski yüksek bir bölgedir. Ancak bölgede gerçekleştirilen jeodinamik çalışmalar ya yetersiz ya da küçük ölçekli kalmıştır.

Bu çalışma bölgede bulunan Tuzla Fayı ve çevresinin bölge tektoniğini daha iyi anlayabilmek için, büyük ölçekli bir araştırma ile izlenmesi ve sonuçlarının değerlendirilmesini içermektedir.

Tuzla Fayı Menderes kasabası ve Doğanbey burnu arasında uzanan KD-GB yönelimli sağ-yanal atımlı bir faydır. Bu fay tarihte üretmiş olduğu depremler ve sınırları içinde bulunduğu İzmir şehrine yakın olması nedeniyle incelenmeye değerdir. Kabuk deformasyonlarının jeodezik yöntemlerle izlenmesi yoluyla yerbilimlerine büyük katkılar sağlayan projelerden esinlenen bu çalışma, çalışılacak bölgenin belirlenmesi amacıyla Ege Bölgesi ve çevresinde günümüze dek gerçekleştirilmiş olan çalışmaları incelemiş, bazılarına da bölge tektoniğinin jeodezi çalışmalardaki önemini vurgulamak amacıyla bu

çalışmada yer vermiştir. Bunun yanında, çalışmanın gerçekleştirileceği bölgede, uluslararası bilimsel platformda kabul görmüş kabuk deformasyonlarını belirleme amaçlı jeodezik ağların tasarımı üzerine gerçekleştirilen çalışmalar bölgede tesis edilen jeodezik ağa uyarlanmıştır. Çalışma bu jeodezik ağ yolu ile gerçekleştirilecek ölçme çalışmaları için de bir veri hazırlama ve değerlendirme adımlarında önerilerde bulunmuştur. Sonuç olarak bu çalışma, kabuk deformasyonları belirlenmesi amaçlı jeodezik bir çalışma için bölge seçiminden veri değerlendirme stratejilerine değin bir dizi önerilerde ve açıklamalarda bulunmaktadır.

TABLE OF CONTENTS

LIST OF FIGURES

LIST OF TABLES

LIST OF SYMBOLS / ABBREVIATIONS

A	Design Matrix
c	Speed of Light
G	Transformation Matrix
H	Locking Depth
n	Number of Stations
P	Pseudorange
Q	The covariance matrix
r_i	Positions of Stations
u	Station Velocity Vector
V	Slip Rate
W	Weight Matrix
x	The Distance Perpendicular to the Fault
Φ	Target Function
CORS	Continuously Operating Reference Systems
GDMRE	General Directorate of Mineral Research and Exploration
TNFGN	Turkish National Fundamental GPS Network

1. INTRODUCTION

In geology science, the term tectonics refers to the processes, structures and landforms associated with deformation of the Earth's crust. In other words, tectonics refers to the evolution of these structures and landforms over time (Keller, and Pinter, 1996).

A catastrophe is defined as any situation in which the damage of the people, property or society in general is sufficiently severe that recovery or rehabilitation, or both are long involved process (Keller, and Pinter, 1996). Great earthquakes can also create catastrophes because of the populated areas and inconvenient materials used in buildings.

Geoscientists have been discussing the idea of large scale continental drift for almost 200 years. However Alfred Wegener was first proposed the detailed theory in 1912. Until the development of the new science paleomagnetism, Wegener's theory was rejected because generally it's thought that the mechanism he suggested was inadequate; the rejection claim that the continents supposedly plowed slowly through the denser oceanic crust under the influence of gravitational and rotational forces. On the other hand, in 1960s, new data from ocean exploration led to the idea of seafloor spreading. Following years made it possible to combine these new concepts under a model called the new global tectonics.

The Earth's lithosphere is divided into a number of large, rigid plates (Figure 1.1.) that move over a layer of the mantle known as the "asthenosphere" and interact at their boundaries. Eurasia, African, and Arabian plates are some of the major plates that interacts each other. They converge, diverge, or slide past one another. Such interactions are believed to be responsible for most of the seismic and volcanic activity of the earth. According to the classical model of plate tectonics, lithospheric plates creep over a relatively plastic layer of partly molten rock known as the "asthenosphere". The

lithosphere as shown in Figure 1.2., which comprises the earth's crust and uppermost mantle, averages about 70 km thick beneath oceans and is at least 125 km thick beneath continents, while the asthenosphere extends to a depth of perhaps 200 km (Monroe, 1996).

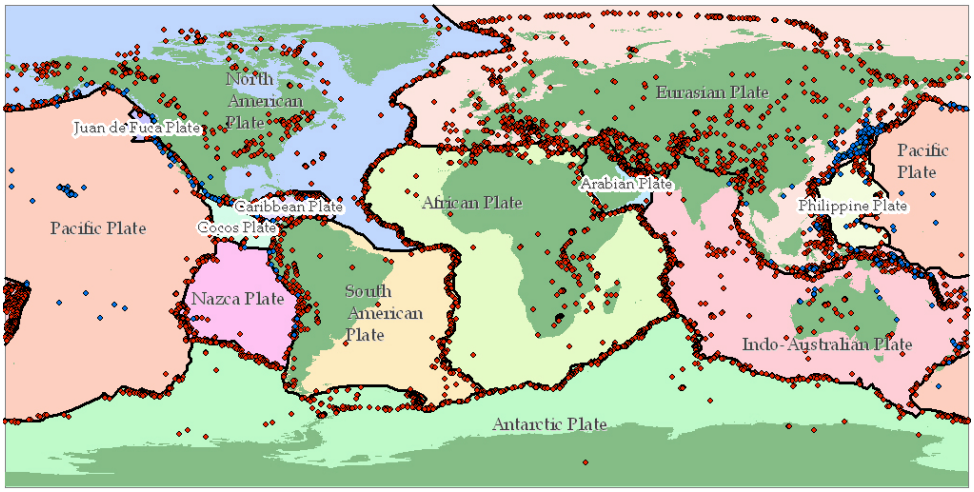

Figure 1.1. Global Plates

Table 1.1. Types of Plate boundaries

Type	Example	Landforms	Volcanism
Divergent			
Oceanic	Mid-Atlantic Ridge	Mid-oceanic ridge with axial rift valley	Basalt
Continental	East African Rift Valley	Rift Valley	Basalt and rhyolite, no andesite
Convergent			
Oceanic-oceanic	Aleutian Islands	Volcanic island arc, offshore oceanic trench	Andesite
Oceanic-continental	Andes	Offshore oceanic trench, volcanic mountain chain, mountain belt	Andesite
Continental-continental	Himalayas	Mountain belt	Minor
Transform	San Andreas Fault	Fault Valley	Minor

Divergent boundaries most commonly occur along the crests of oceanic ridges. Oceanic ridges are thus characterized by rugged topography with high relief resulting from the displacement of rocks along large fractures, shallow-depth earthquakes, high heat flow, and basaltic flows or pillow lavas. Atlantic and Indian oceans are examples of divergent boundaries (Table 1.1.). Convergent plate boundaries are the boundaries where two plates collide and the leading edge of one plate is subducted beneath the margin of the other plate and eventually is incorporated into the asthenosphere. A dipping plane of earthquake foci, called a Benioff (or sometimes Benioff- Wadati) zone, defines a subduction zone. Most of these planes dip from oceanic trenches beneath adjacent island arcs or continents, marking the surface of slippage between the converging plates. Deformation, volcanism, mountain building, metamorphism, earthquake activity, and deposits of valuable mineral ores characterize convergent boundaries (Table 1.1.).

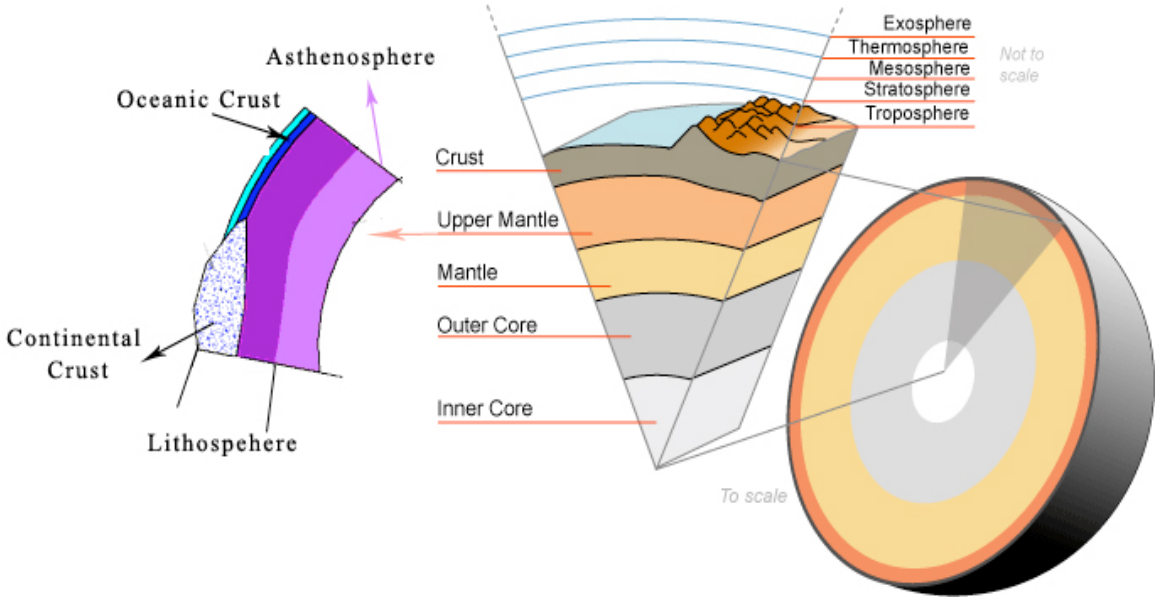

Figure 1.2. The Structure of Earth

Three types of convergent plate boundaries are recognized: oceanic–oceanic, oceanic–continental, and continental–continental. Two oceanic plates converge; one is subducted beneath the other; along an oceanic–oceanic plate boundary. On the other hand, along an oceanic–continental plate boundary, an oceanic and a continental plate converge;

the denser oceanic plate is subducted under the continental plate. Along the continental-continental plate boundaries, two continents collide, they are welded together along a zone marking the former site of subduction. At this type of plate boundaries, interior mountain belt is formed consisting of deformed sediments and sedimentary rocks, igneous intrusions, metamorphic rocks, and fragments of oceanic crust. In addition, the entire region is subjected to numerous earthquakes.

The third type of plate boundary is a transform plate boundary. These mostly occur along fractures in the seafloor, known as transform faults, where plates slide laterally past each other roughly parallel to the direction of plate movement. Transform faults “transform” or change one type of motion between plates into another type of motion. One of the best-known transform faults is the San Andreas Fault in California. Another important transform fault is the North Anatolian fault that lies between the Eurasian and African lithospheric plates and underlie through the Aegean Sea. The relative motions along boundaries are engrossing areas to study for geoscientists because of their possibility to produce catastrophic earthquakes. However, some large scale investigations should be performed in different areas of the country in order to define the risks, encounter the problems and increase the scientific knowledge all around the country.

Deformation measurements by using geodetic techniques include some critical steps, processing and design stages performed in scientific era. Moreover, some other parameters like the location of deformed area or the deformation type that wanted to be determined should also taken into consideration.

A researcher should choose the appropriate technique regarding the deformation type, the closeness of deforming area or object to the urban areas, and the suitable processing techniques.In this project, a large scale deformation study is performed near a high populated city Izmir in the western Anatolia. The study, suggest a schedule for large scale crustal deformation monitoring project including, the relations between the global tectonics, the interpretation of seismicity and tectonics of the study area, appropriate

geodetic techniques for deformation monitoring, combination of different techniques, geodetic network design and optimization, surveying and processing equipment, the theory of measurement techniques and processing and the evaluation of the results.

The second chapter of this study gives some explanations and researches about the study area in terms of the tectonics of region from different studies, considering the geodynamic studies performed in the past. The seismic activity, investigated in order to emphasize the seismic risk of city of Izmir. Historical earthquake information was gathered and processed to analyze the activity of potential faults located near the study area. Important faults were also underlined to give an output for the design stage of the microgeodetic network.

The third chapter suggests the flow chart of the deformation monitoring study and explains the sources of information gathered and present the selected data for network design. This chapter also states some specific approaches for network design taken from several papers (Ayan, 1981, Segall, and Davis, 1997, Gerasimenko *et al.*, 2000, Blewitt, 2000, Shestakov *et al.,* 2003, Taskin *et al.,* 2003). Moreover, this chapter gives information about the microgeodetic network with the parameters effect to the design process. Finally, Izmir Microgeodetic Network is suggested and, site locations and some information about the network is given.

The fourth chapter sets the theory of data evaluation and steps of process for specific software, GAMIT/GLOBK. Some useful tools are introduced in GPS processing. This section also mentions the importance of data collection and pre-processing strategies before getting the adjusted results. Finally, a small recipe is given as an example of GAMIT processing for a particular experiment in UNIX environment.

Following chapters state the future aspects and conclusion.

2. ACTIVE TECTONICS OF WESTERN ANATOLIA

Over the last 200 Ma the Alpine-Himalaya belt represents the most spectacular result of the relative motion between the African and Eurasian plates. The boundary between African and Eurasian plates is delineated by the Hellenic arc and the Pliny-Strabo trench in the west and the Cyprus arc and a diffuse fault system of the Eastern Anatolian Fault Zone in the east (Yilmaz, 2000, Ergun, and Oral, 2000, Kocyigit, 2000, Utku, 2000, Taymaz, 2001).

The Aegean Region and Western Anatolia are one of the most seismically active and deforming parts of Alpine-Himalayan orogenic belt. Thus, a high seismic activity has been observing in this region. An extensional deformation regime has led to subsidence of continental crust over all regions behind the south Aegean. The region is mainly under pure shear stress is an internally deforming counter-clockwise rotating Anatolian Plate relative to the Eurasia.

There is a multi disciplinary project performed for several periods in literature about the plate interactions through the whole Arabia-Africa and Eurasian plates. Figure 2.1. shows the result of this study which is performed by Reilinger *et al.,* in 2006. In the Figure 2.1., CAUC is the Caucasus Block, AN is the Anatolian Plate and AE is the Aegean Plate. Double lines indicate extensional plate boundaries, lines with triangles indicate trust faults and plain lines show strike-slip boundaries. White arrows and adjacent numbers show GPS-derived plate velocities relative to the Eurasia in millimeters per year.

Turkey is situated in the collision zone between the Eurasian, African and Arabian tectonic plates. This collision has resulted in the occurrence of several plate interactions across the country, in particular the Karliova Triple Junction (KTJ) and the North and East Anatolian Fault lines (NAF and EAF), shown in Figure 2.4.

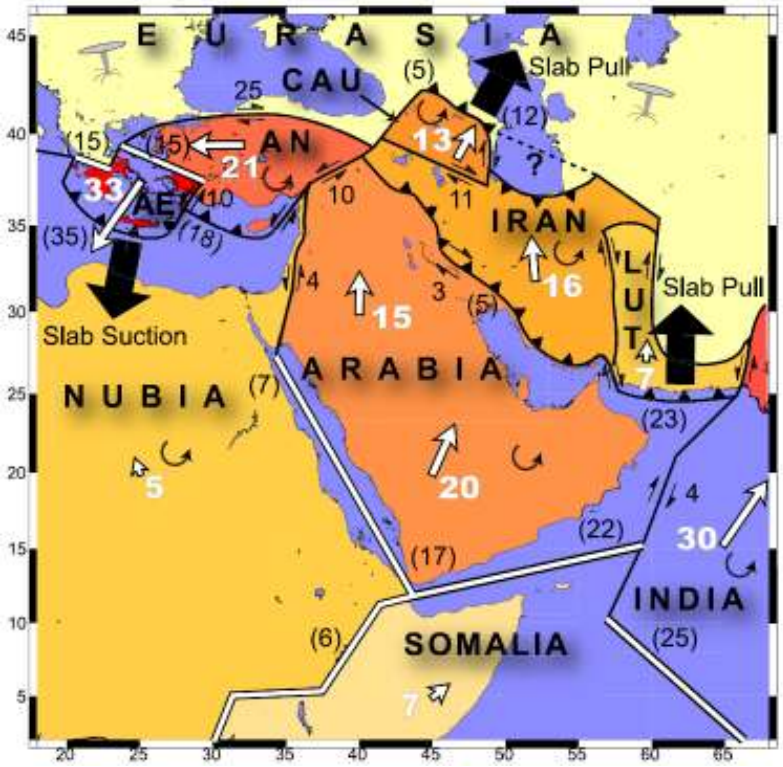

Figure 2.1. Plate interactions of Arabia-Africa-Eurasia zone (Reilinger *et al.*, 2006)

The Aegean Region has been suffering an active N-S extensional tectonics, under the control of two main motions. One of the motions is the westward escape of the Anatolian plate, bounded by the North Anatolian Fault and East Anatolian Fault, intersecting at the Karliova depression of the East Anatolia with a rate of 20-25 mm/yr. the westward motions changes the direction in the West Anatolia with a rather abrupt counter-clockwise rotation, towards southwest over the Hellenic Trench. The other motion is the N-S extension of the Western Anatolia and the Aegean with rate about 3-6 cm/yr. As a result of these motions a group of E-W trending grabens have been developing. These grabens are bounded by E-W trending normal fault zones which, extend about 100-150 km. These fault zones are generally segmented and each segment is no longer than 8-10 km (Yilmaz, 2000).

Marine Geophysics studies produced bathymetric elements of the Aegean Sea, which are the basins that reach to the Aegean Sea from the western Anatolia. These basins are

North Aegean or Anatolian basin, Skiros basin, Psara basin and Ikaria basin. The other important phenomenon of the region is grabens. There are approximately 10 E-W trending grabens in the region. Edremit, Bakircay, Gediz and Menderes grabens are some of them from north to south respectively.

Dynamics of the Aegean Region that is associated with the westward moving Anatolian block would not be the only factor controlling the present day stress field and displacement pattern of the Aegean Region. Although the orientation of the tension may be affected by the Anatolian push, the existence of the tensional stress is due to the forces related to the Crete subduction zone.

Complicated geology of the region also arise the conflicts on the source or beginning of the extension of the region. McKenzie (1988) suggests the beginning time of the extension as 5 Ma. On the other hand, 13-11 Ma is suggested by some other researchers (Angelier, 1979, Mercier *et al.,* 1987). Variety of the suggestions for the beginning of the N-S extension for the Aegean Region may depend on the insufficient accuracy of methods that are used to determine the beginning time or lack of information on the previous geological researches that put the lid on accurate approaches. Consequently, the common belief is to dense the geological investigations on the Aegean Region in order to understand the tectonics of the area. It is certain that, geodesy and geodynamics are also capable to contribute additional information (Segall, and Davis, 1997).

Geodesy, builds its investigations on the information gathered from the seismological studies. Therefore, field studies that aim to define fault traces, interpretation of earthquake distributions and determination of focal mechanisms are valuable data for geodetic crustal deformation study. Thus, the project area that is to be monitored with geodetic techniques has to be evaluated in terms of the project area's seismicity.

2.1. Seismicity

Earthquakes are natural consequences of the dynamic processes forming the ocean basins, continents and mountain ranges of the world. As new lithosphere is produced at oceanic ridge systems, older lithosphere is consumed at subduction zones, or as plates slide past one another. Stress is produced and strain build up in the rocks. Stress defined as the force per unit area on a specified plane, in material such as rocks, and strain is defined as deformation in length or volume, or rapture resulting stress. When the stress exceeds the strength of the rocks, the rupture happens and the energy released in the form of an earthquake.

Table 2.1. Terminology related to the recovery of fault activity (California State Mining and Geology Board Classification)

<table>
<tr><td colspan="3">Geologic Age</td><td rowspan="2">Years Before Present</td><td rowspan="2">Fault Activity</td></tr>
<tr><td>Era</td><td>Period</td><td>Epoch</td></tr>
<tr><td rowspan="3">Cenozoic</td><td rowspan="2">Quaternary</td><td>Historic Holocene</td><td rowspan="5">----200---------
----10,000-------

----1,650,000---
---65,000,000--
4,500,000,000</td><td>Active</td></tr>
<tr><td>Pleistocene</td><td>Potentially Active</td></tr>
<tr><td>Tertiary</td><td>Pre-Pleistocene</td><td rowspan="3">Inactive</td></tr>
<tr><td colspan="3">Pre-Cenozoic Time</td></tr>
<tr><td colspan="3">Age of the Earth</td></tr>
</table>

Most geologists would consider a fault to be active if it has a movement during the Holocene Epoch. The Quaternary Period is the most recent period of geologic time and most of the landscape visible today has been produced during that time. Quaternary Period may be classified as potentially active. Faults that have not moved during the past 1.65 Ma are generally classified as inactive (Keller and Pinter, 1996).

On the other hand, in order to determine a fault as an active fault, paleoseismic studies have to be performed which based on the geologic records. However, according to the security restrictions some agencies state their own classifications for fault behaviour determination. U.S. Nuclear Regularity commission for instance, defines a fault as capable if it has an activity at least once in the past 50 thousand years or more than one in the past 500 Ma.

2.1.1. Seismicity of the Region of Interest

The region has a high seismic activity due to the extensional regime of the Aegean Region. Thus Western Anatolia has a great contribution to Turkey's earthquake activity and neotectonics. Ozmen *et al*., (1997) produced a seismicity map considering the data beginning from the instrumental time to present that indicates the different perspective of western Anatolia than the Turkey's total activity. This difference said to be comes from the seismogenic characteristics of the region. The figure shows the seismic risk zones and the study area is in the high risk-zone I.

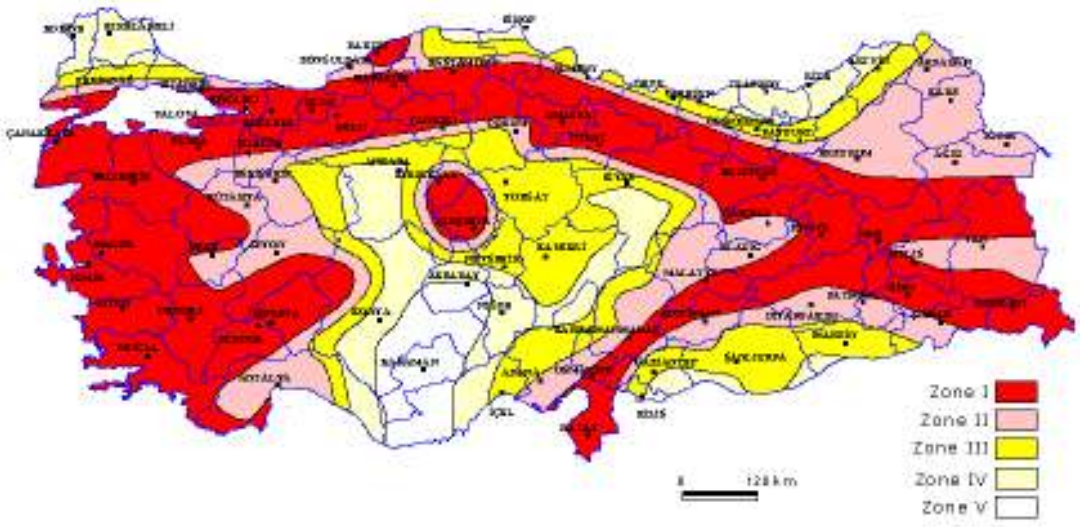

Figure 2.2. Turkey earthquake hazard map (Ozmen *et al*., 1997)

Figure 2.2. can be expressed as numbers in following Table 2.2. The table shows that approximately half of the surface area is under high earthquake risks and about half of the population lives in either highest or high risk zones. Arpat and Bingol (1969) highlighted the E-W trending grabens that had been evolved because of that extension regime like other horsts and grabens.

Table 2.2. Seismic risk zones in terms of population, area, and industry centers and dams distribution in percentages

Earthquake Zone	Population (%)	Surface Area (%)	Major Industry Centers (%)	Dams (%)
Zone I	22	14.8	24.7	10.4
Zone II	39	28.4	48.8	20.8
Zone III	24	28.8	12.0	33.3
Zone IV	20	19.4	12.6	27.1
Zone V	5	8.6	1.7	8.4

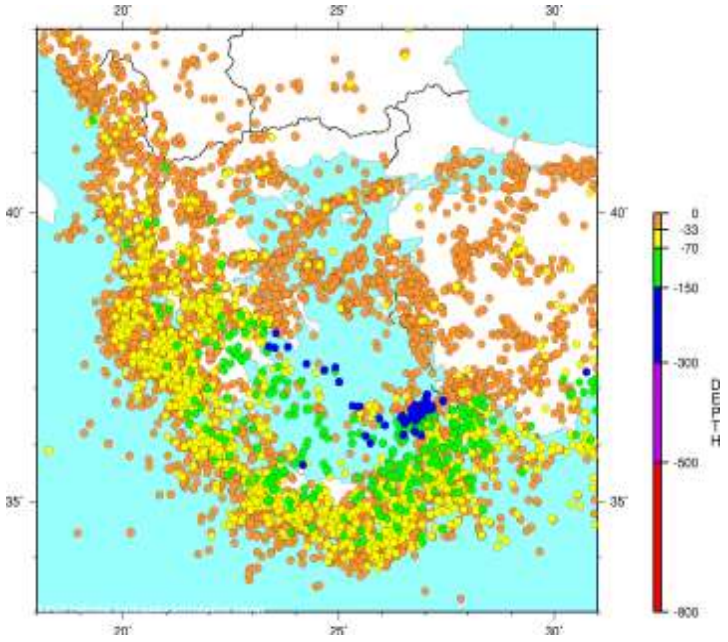

Figure 2.3. Seismicity map of the Aegean Region, M>4 (USGS 1900-2006)

There two main seismic belts within the boundaries of the region. One of them is in a direction of Crete-Rhodes-Fethiye and Burdur and the other one has a direction along Simav-Emet-Gediz and Afyon locations. These two belts have the highest seismicity in the whole Aegean Region (Bagci, 2000, KOERI, and USGS).

Seismic records have been collecting since the beginning of the instrumental time and it is certain that these observations include some errors depending on the seismic network quality, densification and geometry. Faults that produce earthquakes generally have approximately 10 km locking depth and main deformation occurs in the earthquakes that have magnitude greater than 6.0.

2.1.2. General Interpretation

Geodynamic studies show that the Aegean Region needs to be investigated continuously with different scientific techniques. This study is going to subject the geodetic contribution to regional tectonics with some geodetic optimization techniques using gathered information from different sources. Although the tectonics of Eastern Mediterranean explained with the long term episodic and continuous GPS observations (Reilinger *et al.,* 2000, Reilinger *et al.,* 2006) some special cases need to be defined in specific regional deformations. Izmir as a high populated city had settled on seismically active faults. Thus, there is always high seismic risk underlined in many studies (Ozcep, 2002, Ozcep *et al.,* 2003, Nur, A., and Cline, 2000, Kreemer, and Chamot-Rooke, 2004, Aktug and Kilicoglu, 2006, Zhu *et al.,* 2006a, Ocakoglu *et al.*, 2005a) in Izmir like the North Anatolian Fault Zone.

There are also several GPS network optimization studies (Blewitt, 2000, Gerasimenko *et al.,* 2000, Wu *et al*., 2003) published during last decade. Therefore, there is a need to perform a large scale crustal deformation monitoring study by using the results of previous studies mentioned above in order to contribute regional tectonics. However, the

tectonics of Izmir and its vicinity is very complex in geological sense and should be investigated in detail to understand long and short term geodynamic activities. Thus, considering the close relationship between geodynamic and geodetic phenomenon, following topic gives some information about tectonic evolution of Izmir and surrounding area.

2.2. Tectonics of Izmir and its Vicinity

The deformation pattern in the Mediterranean region which constructs a low elevated part of the Alpine Himalayan belt is rather complex, and usually occurs in continental collision zones. The Aegean region is bounded to the north by the stable continental Eurasian plate, to the west by the Adriatic region, to the east by the central Anatolian, and to the south by the oceanic material beneath the Mediterranean Sea which is northern edge of the African plate. Black and Mediterranean Sea floors with mean depth of 1500 and 1300 meters successively, the Aegean Sea floor has a mean depth of 350 m. In other words, the Aegean Sea floor is seen as a high plateau between the deeper Black Sea floor and Mediterranean Sea floor. The Aegean is characterized by a relatively thicker crust (25-30 km) than a typical oceanic crust, which might be interpreted as a thinned continental crust.

The Aegean is also situated in the convergent boundary between the African plate and Eurasian plate. The African plate has rotated counter-clockwise with respect to Eurasian plate during the last 92 Ma (Müller *et al.,* 1997). The spatial distribution of earthquakes and detailed topographic studies indicate the existence of a northward-dipping subducted slab beneath this region (African plate beneath Eurasian plate). However, according to Müller *et al.,* (1997) roughly N-S directed lithosphere shortening rate is increasing from west to east in the Aegean region. The region is also characterized by high heat flow, which is related to thin and deformed (stretched) continental crust. This thinning is continuing till now and for this reason, it is the world wide most seismically active and

internally deforming area of the entire Alpine-Himalayan belt and at of all continents (Sodoudi, 2005, McKenzie, 1972; Mercier *et al.*, 1989; Jackson *et al.*, 1994).

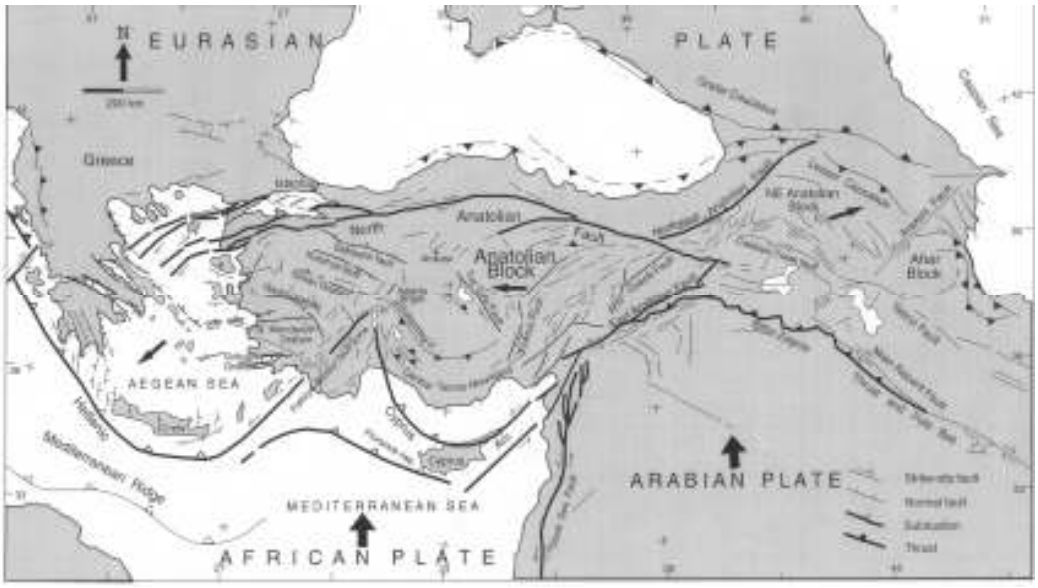

Figure 2.4. Active tectonics of Anatolia (Barka, and Reilenger, 1997).

Figure 2.5. shows the main geological futures of the Aegean Region. Papazachos (1999) defines the northern and eastern boundaries of the Aegean plates as dashed lines marked on the figure. The arrows indicate the relative motion with respect to the Eurasian Plate defined by McClusky *et al.,* (2000), and the rectangle shows the study area approximately.

The focal mechanism solutions of earthquakes indicate that the faulting in the western part of the Aegean region is mostly extensional in nature on normal faults with a NW to WNW strike and slip vectors directed NW to N *(Taymaz, 2001)*. The evidences from paleomagnetism show that this region rotates clockwise relative to the stable Eurasia. According to Piper *et al.,* (2001), paleomagnetic data in the eastern Aegean Region is consistent with very small or no rotations in the northern part and possibly counter-

clockwise rotations in the south relative to the Europe, including some ambiguities. The strike-slip faulting that lying through the central Aegean from the east appears to end abruptly in the SW against the NW trending normal faults of Greece (Figure2.5.).

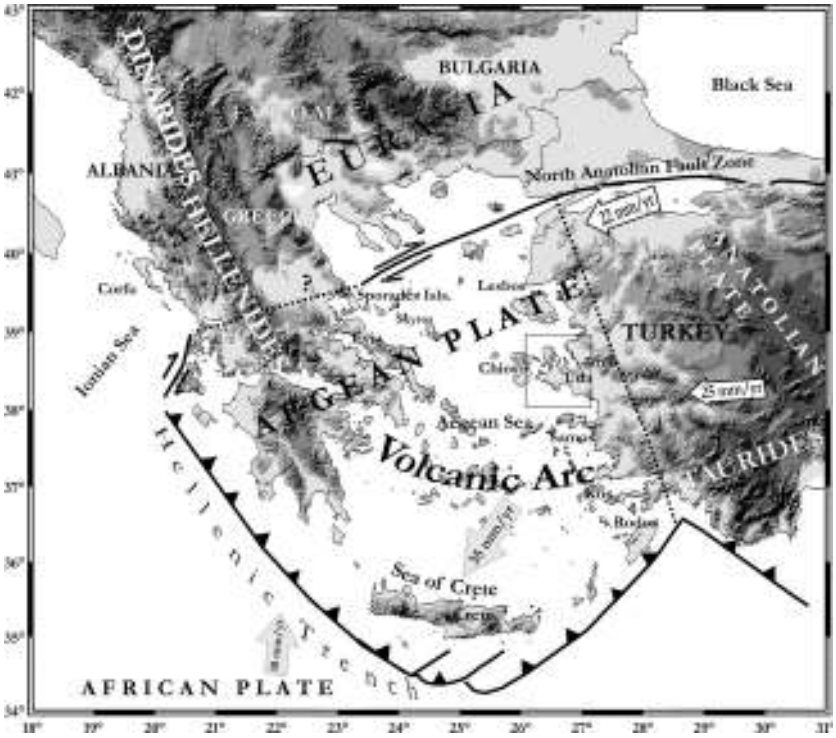

Figure 2.5. The compression and extension zones in the Aegean Region (Black rectangle shows the study area), (Papazachos, 1999).

The kinematics of the Aegean region is generally defined with the interaction of a few geodynamic phenomena. The westward motion of Anatolia, the continental collision between NW Greece-Albania and the Apulia-Adriatic platform in the west and the Hellenic subduction zone to the south perform the kinematics of the Aegean. The right-lateral slip on the North Anatolian Fault distributed to several parallel faults in the Aegean Region.

According to McKenzie (1972) the westward motion of Turkey relative to Eurasia was accommodated by the shortening in the Hellenic trench, as southern Aegean overrides the Mediterranean Sea floor. For this reason McKenzie claims that the strike-slip faulting associated with the NAF continue through the north Aegean and central Greece to link up the northwestern end of the Hellenic Trench system but, this not the case. The faulting systems are too complex to be defined as a single strike-slip approach. McKenzie (1978), claim that there is no single strike-slip fault with a NE-SW strike in central Greece. On the other hand, tectonics is dominated by normal faulting with a WNW-ESE strike. Consequently, the first thought of McKenzie is not false but it is simplistic. There is a complicated motion with a NE-SW trend, which must cross central Greece and the north Aegean involving rotation of block in both horizontal and vertical. GPS velocity fields, SLR observations, seismic moment rates and kinematic arguments assert present deformation estimates, related the tectonics of the region. Taymaz (1991) explains the region tectonics by a simple experience. A simple two-dimensional analogue of this deformation style described with a book example.

Consider a book or magazine with a flexible cover such as telephone book. According to example of Taymaz, if the book has no binding, so that it is simply stock of parallel paper sheets, than distributed sample shear, such that the edge CD rotates to CD', is accomplished by sliding parallel sheets over each other. Than the left hand edge rotates from AB to AB`. The sheets do not rotate and the deformation resembles distributed strike-slip faulting on parallel faults. If the book has a binding such that the left hand edge AB in Figure 2.6., that the distributed simple shear on the right hand edge causes deformation (movement to D to D') as seen in the figure. In this condition the strike-slip faulting occur only on the right hand side. On the other hand, towards the centre gaps appear between the sheets, and also it bulges out towards the bottom of the picture.

Taymaz (2001), claim that the gaps represent extension perpendicular to the top of the picture which is the line AC and accompanies overall shortening in the orthogonal direction. In the case of Figure 2.6., drawing three, this style of deformation arises because

of the binding of the book is rigid and con not change length which means AB in the figure must equal to the AB'.

However, the same style of deformation arises because the binding of the book is rigid and cannot change length, but does not rotate as fast as CD. The stretch in the figure resembles the rotation in Aegean Region in several ways. Right-lateral strike slip faulting on faults that change in strike form from ENE to NE dominate the eastern side. Normal faulting with a WNW to NW strike is prevalent in the west and responsible for the growth of the basins in the Aegean Region. The black gaps in the book example resemble the basin in the region. The structures start to rotate when they reach the region where there is N-S extension. In the west, the sense of rotation is clockwise, but in the east the rotation is counter-clockwise. Taymaz (2001) gives a point to possibility that the counter-clockwise are related to the rotation of the big strike slip faults, whereas the clockwise rotations caught up in the right-lateral shear between them.

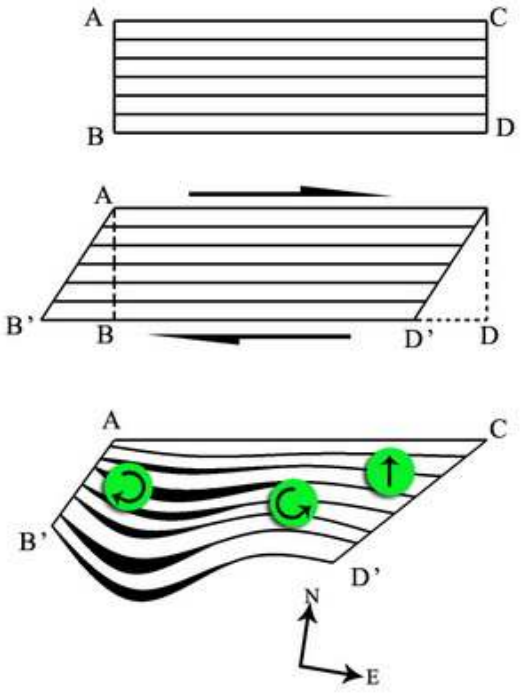

Figure 2.6. Sketch illustrates a simple analogue deformation in the Aegean Region

Finally, the principle effects that dominate the active tectonics of the Aegean can be described in three main topics. The first effect is the westward motion of Turkey relative to Europe (Eurasia lithospheric plate). This westward motion is accommodated by localized slip on the NAF in central Anatolia, but distributed right-lateral shear in NW Turkey, the Aegean Sea and Thrace. The second principle effect is the collision between the Albania-Greece margin and the Apulia-Adriatic platform in the west which leads the continental shortening of the crust. Moreover, the collision also leads the consequent resistance to the rotation of Greece and Albania that is necessary to take up the distributed right-lateral shear. Another effect is the subducted lithosphere slab beneath the southern Aegean, which generates extension in the lithosphere above it as it sinks into the mantle (Taymaz *et al.,* 1991, Taymaz *et al.,* 2001).There is a dramatic change in the character of deformation from east to the west through the whole region. The change is mainly has a strike-slip trend in the east and mainly normal faulting in the west. This change is related to the failure of the western seaboard of the Greece and Albania to rotate rapidly enough to accommodate the westward motion of Turkey. Moreover, it is initiated with the extension in the Aegean Sea that causes its southern margin to override the oceanic crust of Mediterranean, and leading to the establishment of a sinking slab and helps the sustain the deformation.

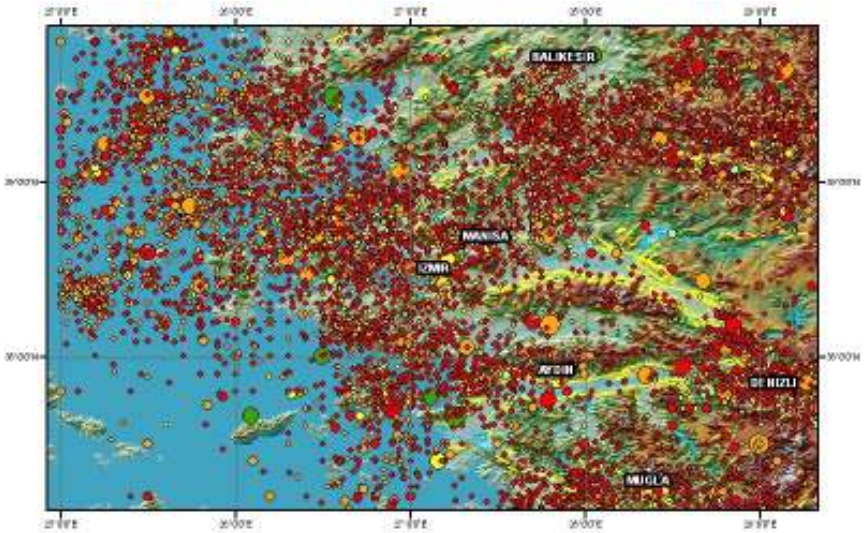

Figure 2.7. Seismicity of Izmir and its vicinity, M>3 (Earthquakes 1900-2006 KOERI)

2.2.1. Important Faults

The extension tectonic regime effect the Western Anatolia in the neotectonic age. Izmir is established in the west side of the Gediz Graben and bound the gulf of Izmir. There are several active faults that trigger the dense earthquake activity recorded beginning from the 20th century as shown in Figure 2.7. In addition some major faults, which are described in following paragraphs, have possibility to produce big earthquakes (Figure 2.8.). According to the report on Active Faults and Seismicity in Izmir and its vicinity (Emre *et al., 2005*), there is not enough investigations on the earthquake activity potential except Gediz graben. The report, define active faults within a 50 km semi-diameter area which has an origin at central Izmir. Emre *et al.,* (2005) defined 14 active faults (Figure 2.9.) through the region. These faults are Guzelhisar, Menemen, Yenifoca, Izmir, Bornova, Tuzla, Seferihisar, Gulbahce, Gumuldur, Gediz Graben detachment faults, Daglikizca, Kemalpasa, and Manisa Faults. Fallowing paragraphs are going to give brief explanations about these active faults and focus on Tuzla Fault in detail.

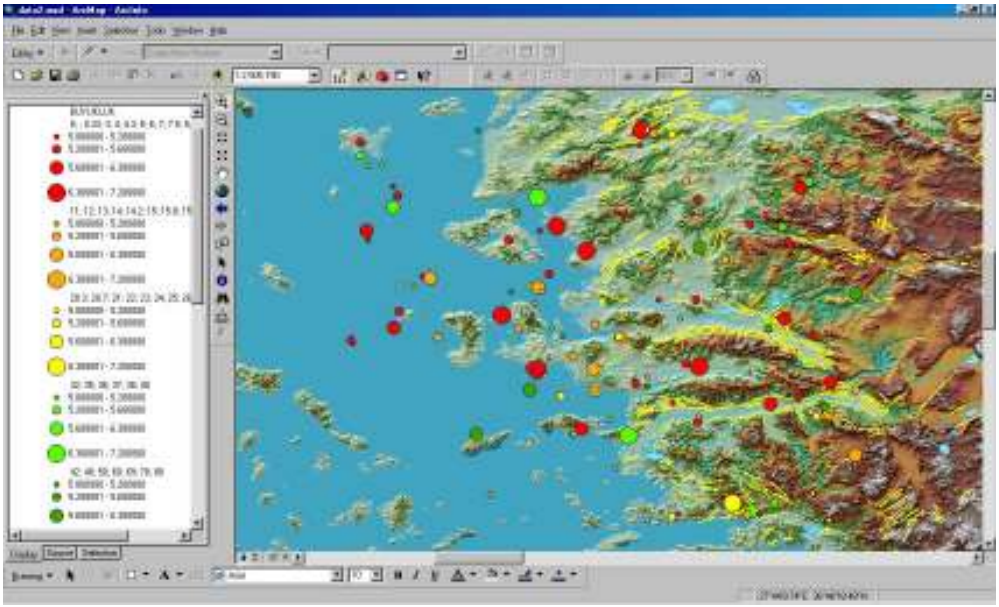

Figure 2.8. Faults and earthquakes, M>5 in 1900-2006 KOERI

Guzelhisar fault is lying in the north of Izmir between Aliaga and Osmanlica counties. The fault is approximately 25 km long. The field investigations (Emre *et al.*, 2006, Saroglu *et al., 1985*) claim that the fault has a right lateral strike-slip character. According to the geomorphologic evidences, Guzelhisar Fault was active in Quaternary period.

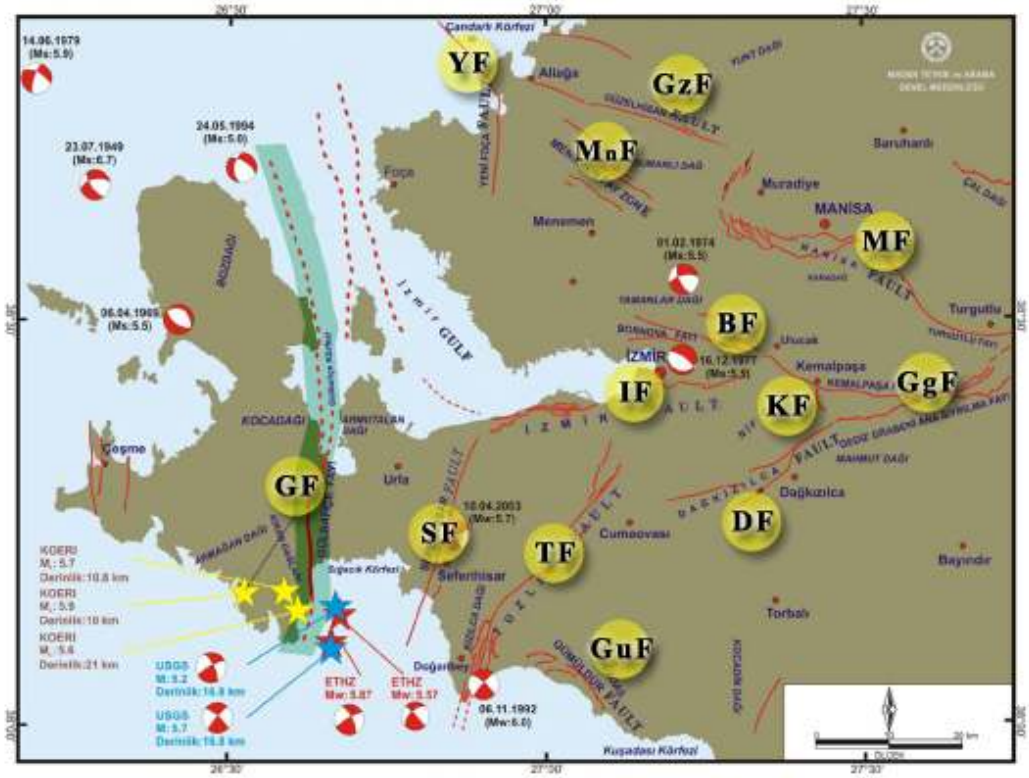

Figure 2.9. Important faults of Izmir and its vicinity (Emre *et al.,* 2005) (GF: Guzelhisar Fault, MnF: Menemen Fault, YF:Yenifoca fault, IF: Izmir Fault, BF: Bornova Fault, TF: Tuzla Fault, SF: Seferihisar Fault, GzF: Gulbahce Fault, GuF: Gumuldur Fault, GgF: Gediz Graben Detachment Faults, DF: Daglikizca Fault, KF: Kemalpasa Fault, MF:Manisa Fault)

The faults that lying between Dumanlidag volcanoes and Gediz lowlands and has a direction of NW- SE, are called Menemen Fault Zone. The length of the zone is 15 km and its wide is 5 km. There is no certain evidence about the detail characteristics and activity, of the faults in quaternary period, although the traces of these faults can be easily

appreciable from aerial photographs. Because of the lack of information and the uncertainty of the quaternary activity these faults are marked as possibly active by the General Directorate of Mineral Research and Exploration.

Yenifoca Fault is lying at the east of Yenifoca county between the port of Nemrut and Gerenkoy at the south with a lineament trending N-S. It is approximately 20 km long. Yenifoca fault is a left-lateral strike slip fault and defined as potentially active fault.

According to Emre and Barka (2000), Izmir fault is lying in the east of gulf of Izmir and it is a morphologic boundary of that gulf with a lineament of E-W. Izmir fault is a dip slip normal fault with a length of 35 km. the fault is lying through the city centre and composed of two segments. Each of the two segments is 15 km long. According to the information reported by General Directorate of Mineral Research and Exploration (GDMRE), Izmir fault is an active fault during the Holocene period with surface raptures.

Bornova Fault is in the northeast of Izmir and west of Karsiyaka with a lineament trending of NW-SE and composed of several parallel faults. There is not enough information gathered in order to evaluate these faults as active faults related with their activity during the quaternary period.

Another important fault is the Seferihisar Fault lying between gulf of Sigacik and Guzelbahce with a lineament trending of N20E. According to Ocakoglu *et al.,* (2005b), this fault has continuity through the Aegean Sea to the south. Seferihisar fault is 23 km long and if the undersea segments are considered the total length is approximately 30 km (Emre *et al.,* 2005). According to the observations of Inci *et al.,* (2003) the fault defined with its right-lateral strike slip behaviour. Result of the focal mechanism solutions performed by Tan and Taymaz (2003) after the 10^{th} of April, 2003 earthquake, designate a NE-SW right-lateral trend for the fault trace. Seferihisar fault has a connection to E-W trending Izmir fault so the fault can be evaluated as a transfer fault of Gediz garaben system like Tuzla fault.

There is an important fault line, separating the Karaburun peninsula in terms of its morphologic and structural properties, called Guzelbahce fault. The fault is also known as Karaburun fault in some publications. It has a length of 70 km including the segments under the sea (Ocakoglu *et al.,* 2005b). The fault is composed of two segments of the fault which are 30 km long south segment and 40 km long north segment. Investigations in Ocakoglu *et al.,* (2005a) show that strike-slip dominant behaviour. On the other hand, there are also some oblique components on the north segment of the fault.

Gumuldur fault is lying between Gumuldur and Ozdere counties in the southwest of Izmir with a lineament trending of N55W. It has a length of 15 km and normal faulting behaviour. Gumuldur fault marked as a potentially active fault because of being a boundary to the gulf of Kusadasi and its effect on the morphology of quaternary. Gumuldur fault is lying in the southeast of Tuzla fault.

Tuzla fault is in the southwest of Izmir, between Doganbey cape and Gaziemir counties with a lineament trending NE-SW. It has different names in the literature such as Cumaovasi and Orhanli faults (Emre and Barka, 2000, Saroglu *et al.,* 1992). The fault is 42 km long through the land side. However, in 2004 and 2005 the after the investigations performed by GDMRE Sismik-1 research ship in Doganbey cape the total length published as more than 50 km. Tuzla fault is defined as three main segments that have different directions. Emre *et al.,* (2005)., named these three parts as Catalca, Orhanli and Cumali sections arranged from north to south respectively. The segments are shown in geology map in Figure 2.11.

Catalca that forms the northeast section of the fault is 15 km long and has a lineament trending of N35E. This section is separated with a 750 m bounce to the right hand side to the other section; Orhanli. The Catalca segment of the Tuzla fault has right lateral strike slip behaviour. Orhanli segment that is placed in the southeast of the Tuzla fault has a lineament trending of N50E and 16 km long.

The last segment, Cumali has a zonal structure with a lineament of NNE-SSW trend and composed of several parallel faults. This fault zone is between Cumali thermal springs and Doganbey cape with a length of 15 km. Moreover, according to the studies performed by Ocakoglu *et al*., (2005b), the fault zone continues through the base of the Aegean Sea. The total length of this zone is approximately 25 km. The faults in this zone are generally had lineament trending of N20E except the fault that is evaluated as inactive on the western boundary of the zone.

Other important faults of the region are Gediz graben detachment faults (normal faults with a lineament E-W), Daglikizca fault (13 km long right-lateral strike-slip fault with a lineament trending N65E), Kemalpasa fault (24 km long normal fault with a lineament N75E) and Manisa fault (40 km long normal fault with a lineament trending N65W). In 1992 there is an earthquake was occurred 6.0 magnitude (Figure 2.10.) between Izmir and Doganbey with a depth of 14 km. the focal mechanism solutions show that the epicenter of that earthquake was in the Aegean Sea near Doganbey cape and the after shocks of the earthquake were distributed on Tuzla fault. According to the fault plane solutions of Turkelli *et al*., (1995) the right-lateral strike slip mechanism evolved the earthquake.

Therefore, the right-lateral strike slip Tuzla Fault, with its 50 km length (including the undersea segments) is considered as an active and important tectonic phenomenon of Izmir and its vicinity.

On the other hand, Tuzla Faults is the main element that defines the paleo-geography of the region during the Miocene period (Genc *et al.,* 2001). Genc *et al.,* also claims that the fault has left-lateral strike slip behaviour. In contrary, some other studies (Emre *et al.,* 2005, Barka *et al.,* 2000, McClusky *et al.,* 2000) propose that the fault has a right-lateral strike slip behaviour during the quaternary. The fault plane solutions determined by Turkelli *et al*., (1992, 1995) also confirm this theory.

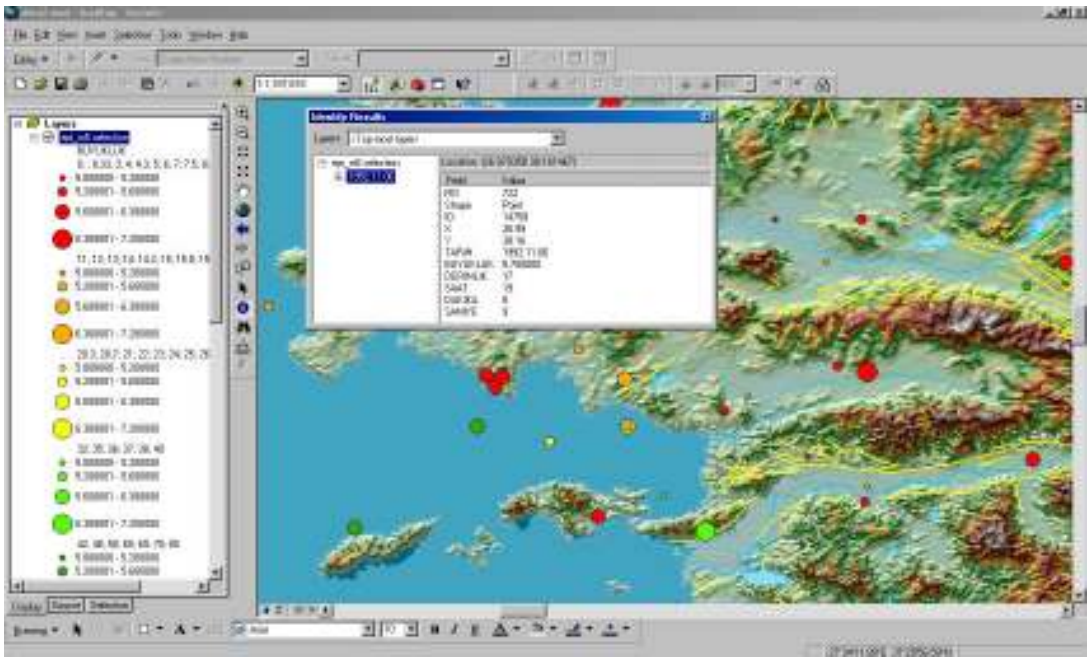

Figure 2.10. June, 11, 1992 earthquake, Tuzla fault (KOERI)

Figure 2.11. The Geology map of Izmir-Doganbey

2.2.2. Important Historical Earthquakes

Western Anatolia hosted many civilizations on the eastern lands of the Aegean for millenniums. Moreover, the region was a centre of trade and intellectual life and lots of scientific developments performed during those periods. For this reason, western Anatolia has a lot of information gathered in many issues such as earthquakes. That is why this region has very precise earthquake information for almost 2000 years. However, earthquake databases recorded with instruments since 1900 so the whole period divided into two periods. Historical period, including the records beginning from 1900 up to epoch 1990, and instrumental period includes records beginning from 1990 to present. Table 2.2. and Table 2.3. show important earthquakes recorded in these periods. According to the historical records the earthquake happened in 17 A.C. destroyed 13 Ionian cities including the Ephesus. This is the most important and catastrophic earthquake in the entire Aegean Region. Another important earthquake happened in 688 and records had reported that 20000 people had died. During the instrumental period there are also many important earthquakes near Izmir. For instance, in 1928 M:6,5 Torbali earthquake damaged more than 2000 buildings. 1992 Izmir Mw: 6,0 and 2003 Urla Mw: 5,7 earthquakes have damaged the buildings. Faults of the study area and some important earthquakes and their focal mechanism solutions shown in Figure 2.12. and Figure 2.13.

Table 2.3. Catastrophic earthquakes in the region (Historical Period)

Day	year	lat	lon	int	M
	17	38,40	27,50	X	7,0
	105	38,90	27,00	VIII	6,4
	176	38,60	36,50	VII	5,8
	177	38,60	36,50	VII	5,8
	178	38,30	27,10	VIII	6,5
	688	38,41	27,20	IX	6,5
	1039	38,40	27,30	VIII	6,8
20.Mar	1389	38,40	26,30	VIII	6,7
20.May	1654	38,50	27,10	VIII	6,4
02.Jun	1664	38,41	27,20	VII	5,8
	1668	38,41	27,20	IX	
14.Feb	1680	38,40	27,20	VII	6,2
10.Jul	1688	38,40	36,90	X	6,8
13.Jan	1690	38,60	27,40	VII	6,4
Sep	1723	38,40	27,00	VIII	6,4
04.Apr	1739	38,50	26,90	IX	6,8
24.Nov	1772	38,80	26,70	VIII	6,4
03.Jul	1778	38,40	26,80	IX	6,4
13.Oct	1850	38,40	27,20	VIII	
03.Nov	1862	38,50	27,90	X	6,9
01.Feb	1873	37,75	27,00	IX	
29.Jul	1880	38,60	27,10	IX	6,7
15.Oct	1883	38,30	26,20	IX	6,8
01.Nov	1883	38,30	26,30	IX	

Table 2.4. Important catastrophic earthquakes in the region (Instrumental period)

Day	year	lat	lon	depth	intensity	M
19.Jan	1909	38,00	26,50	60	IX	6,0
31.Mar	1928	38,18	27,80	10	VIII	6,5
22.Sep	1939	39,07	26,94	10	IX	6,6
23.Jul	1949	38,57	26,29	10	X	6,6
02.May	1953	38,48	26,57	40	VIII	5,0
16.Jul	1955	37,65	27,26	40	VIII	6,8
19.Jun	1966	38,55	27,35	9	VIII	4,8
06.Apr	1969	38,47	26,41	16	VIII	5,9
01.Feb	1974	38,55	27,22	24	VIII	5,3
16.Dec	1977	38,41	27,19	24	VIII	5,5
14.Jun	1979	38,79	26,57	15	VIII	5,7
06.Nov	1992	38,16	26,99	17	VIII	5,7
28.Jan	1994	38,69	27,49	5	VIII	5,2
24.May	1994	38,66	26,54	17	VIII	5,0
10.Apr	2003	38,26	26,83	16	VIII	5,6

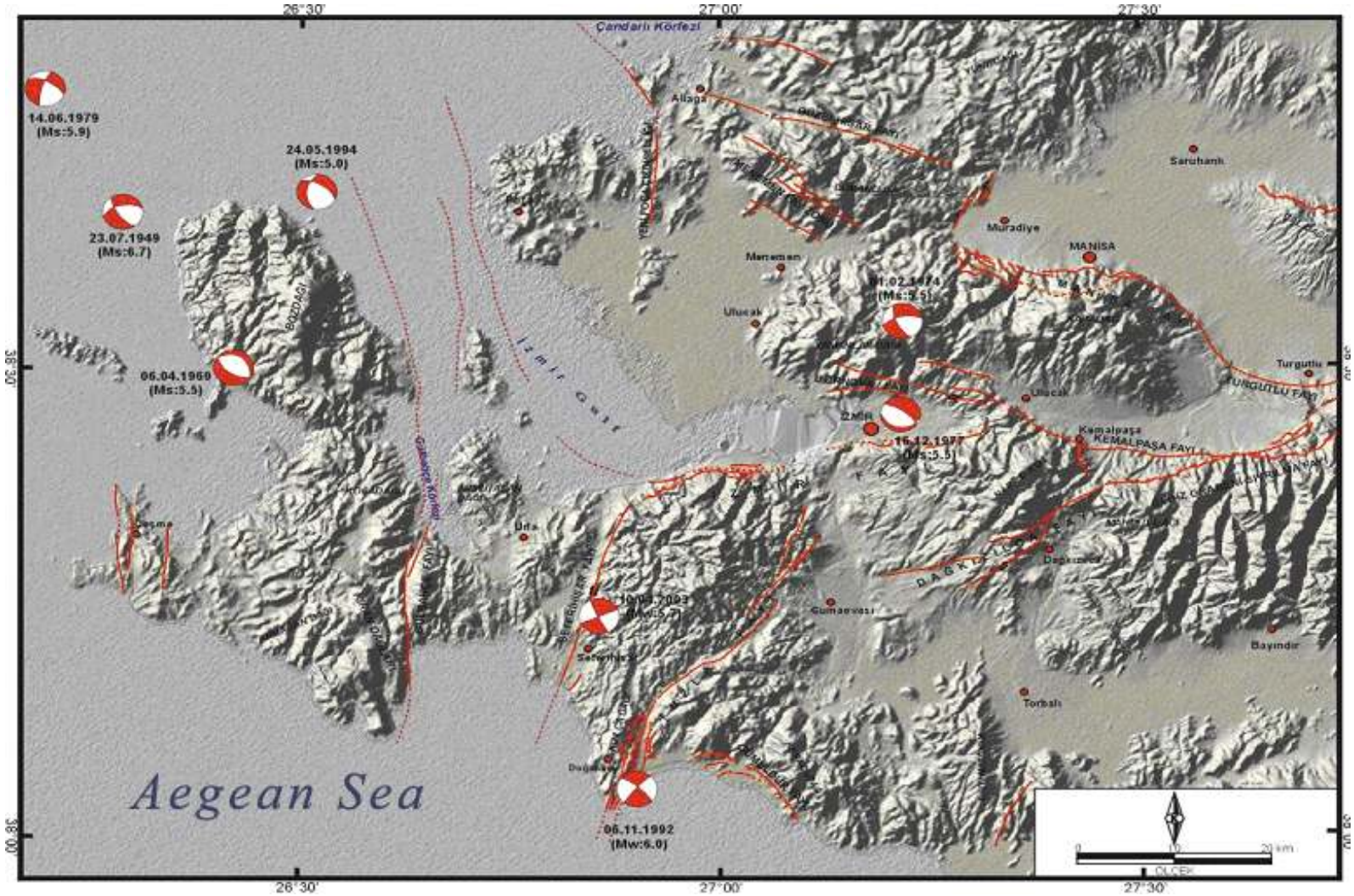

Figure 2.12. Faults of the study area-Izmir and its vicinity with focal mechanism solutions of some important earthquakes (Emre *et al.,* 2005, McKenzie, 1972; Turkelli *et al.*, 1995)

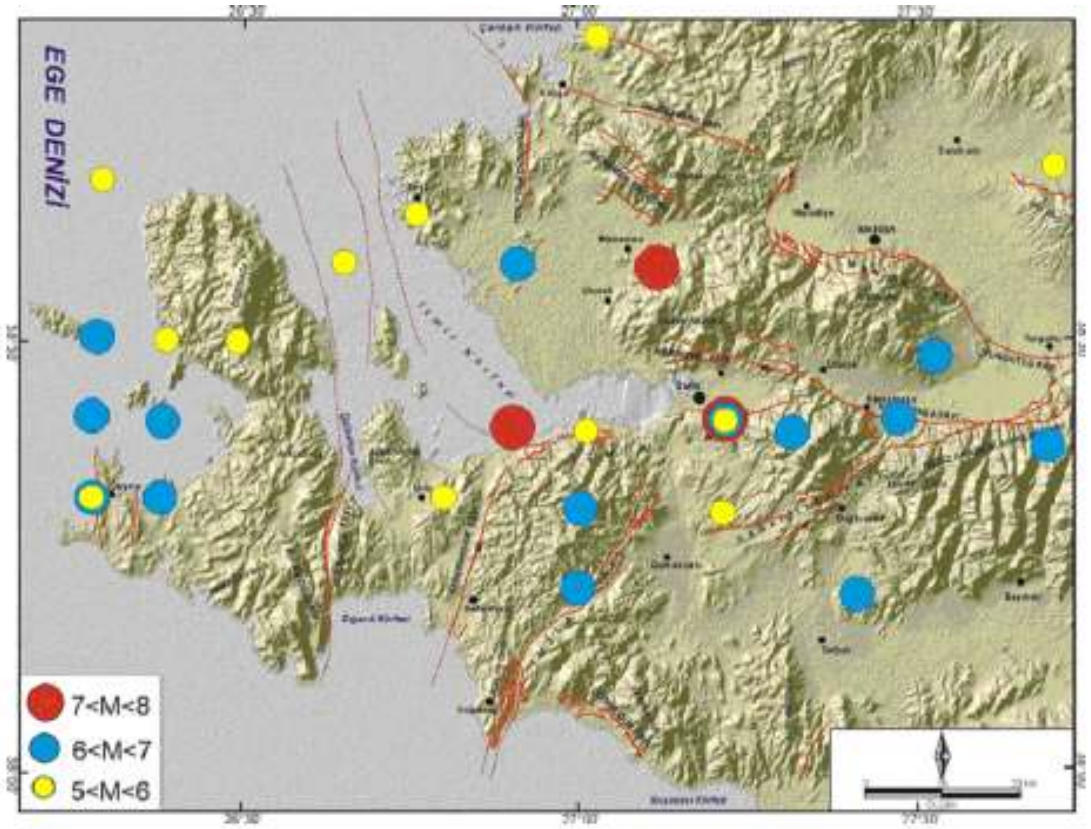

Figure 2.13. Some historical earthquakes, M>5

3. DESIGN AND IMPLEMENTATION

In the past, high precision was desired only in national geodetic networks. However, nowadays, not only in crustal deformation studies, but also in engineering studies, dam deformations, applications in large constructions and industrial equipments, complicated projects and even in archaeological and architectural applications there is a need to achieve high precision. Conventional geodetic techniques loosing its importance in many application areas with the wide spread usage of the satellite techniques. Ease use in practice, cheap equipment, and advanced processing techniques evolve surveying applications to the satellite based observations. Moreover, continuously operating reference systems (CORS) support the use of GPS technique. On the other hand, CORS generally do not give sufficient performance for monitoring crustal deformation because of the insufficient control point density of the system. Thus, for small area or fault based large scale studies needs to be optimized in terms of following expressions.

Observation techniques, selected equipment and surveying interval of any project have to be optimized in terms of some parameters. These optimizations, in general, are realized to achieve a desired precision. Besides, reliability is also as important as precision. One should trust not only the results but also the reliability of a network which can be expressed as mathematical relations. The precision, reliability and economical parameters in a geodetic network can be arranged in order to achieve the optimum solution which is defined as the optimization of geodetic networks (Ayan, 1981).

In order to determine the deformation, generally local networks are preferred. Deforming area generally covered by a number of control points. These points constitute a geodetic network and their location or structure is defined by the topographic and geological parameters. The number of points is directly related with the deforming object and the deformation accepted in the area. The ideal approach is an interdisciplinary study to define the number of points and locations for these “control networks”. Ayan (1981)

suggested three sets of control points for deformation monitoring which are deformation points, reference points and orientation points.

In order to design a monitoring network along Tuzla Fault-Izmir, some pre-studies were performed. This chapter focused on the stages and a general schedule for the whole study. First of all, some information is gathered from several sources such as internet, municipalities, General Directorate of Land Registry and Cadastre, Bank of Province, some surveying companies, and personal communications. As a result of these communications, numerous data have collected. Thus, an evaluation and elimination process is needed. Then, the theory of network design is stated according to the approaches of some researchers who deal with the geodetic network design including geophysical parameters. Some additional information introduced from several studies and experiments which deal with the station numbers and locations in a control network. Some results from different studies reevaluated and adapted to the study and shown in following sections.

Finally the Izmir microgeodetic network introduced according to the suggestions stated by several geoscientists and experiments. The coincidence between these studies and our study discussed and the compatibility was underlined.

3.1. Gathered Information

Collecting necessary information settled on the literature researches. Geophysical, geologic, geodynamic, and geodetic experiments and studies were collected both from internet, scientific journals, books, and personal communications. Collected documents show that there are lots of geophysics and geologic studies all around the western Anatolia and also around Izmir. The density of the scientific researches performed in this region can be explained with the intensive seismic activity of region and catastrophic earthquakes.

However, despite the dense geodynamic researches performed in this region, geodetic investigations are limited or small scaled.

In order to contribute geodynamic studies, after Sigacik earthquake 2005 with M:5.9, this region's seismic risk had considered. As mentioned in Chapter 2, Izmir has a very complex geological structure of faults with different characteristics. This variety in fault characteristics also made it difficult to select the project area. For this reason, at the beginning the information collected about the region had covered the whole western Anatolia but then the researches had focused on the most important section of the region. Tuzla Fault and its neighborhood coincide with the aims defined at the beginning of the study because of the active behaviour of the fault, its closeness to Izmir and big earthquakes recorded in the area.

Geodetic deformation analysis requires a stable, continuously or periodically observed network. Moreover, in order to estimate the small amount of deformations, some additional techniques are generally taken into account. This project, which focused on the Tuzla fault, designed a micro-geodetic network considering the valuable information gathered from different resources such as municipalities and then state the theoretical background with some scientists' approaches in terms of geodetic optimization.

The general plan for the network design performed on several parameters which are the available data collected from local resources, the topographic and economic situations, equipment which is going to be used and the fault geometry. The outputs of these parameters are the approximate locations of the geodetic control points, the number of the stations, and the observation and processing strategies.

First of all, examples of network design and optimization projects' results were investigated. Then, the necessary information, such as the locations, types and availability of national control stations of the region, gathered from local administrations. Izmir

Manucipility of Greater City, Bank of Provinces, and Seferihisar branch of General Directorate of Land Registry and Cadastre were the main sources for valuable information. Because of the high cost of constructing control points, existing stations were preferred to be used. On the other hand there is also an open end establishing additional stations where necessary. Figure 3.1. shows all of the geodetic control points collected from the resources mentioned above. Some of them belong to the Turkish National Fundamental GPS Network (TNFGN) (PAYM, BIST, KNRL, GMDR, DBEY, and SFRH), so they have much more possibility to be chosen as network stations because they are widely used for various applications and have monument stabilities (most of them are pillars).

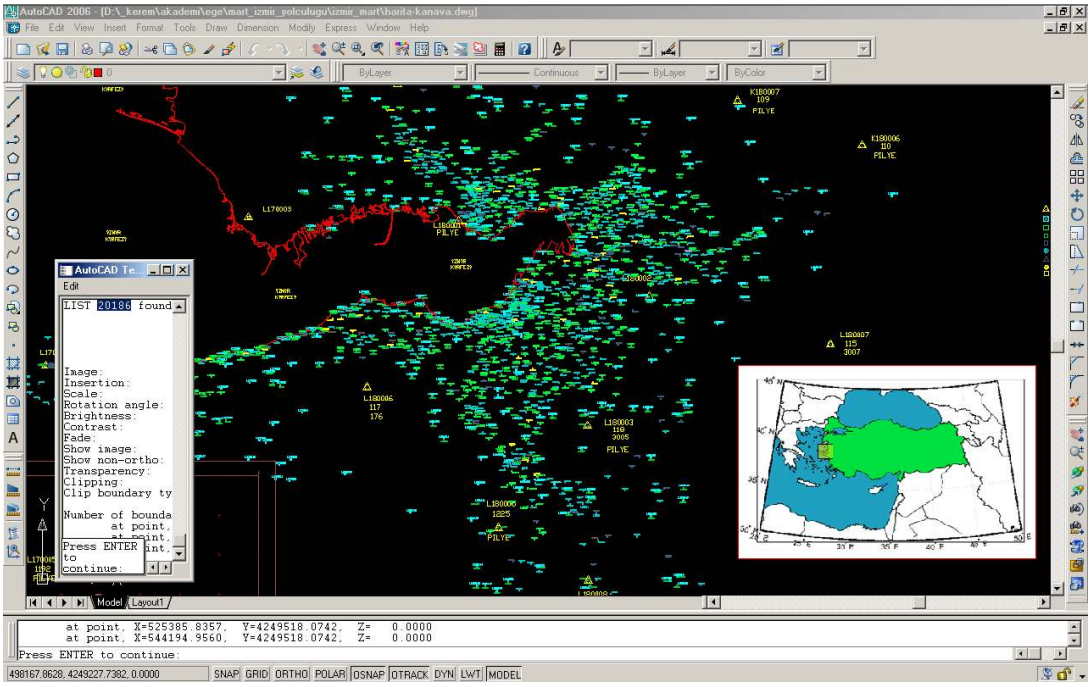

Figure 3.1. Set of control points established to the study area

The theory of network design should be mentioned in terms of geophysical parameters before the suitable control points are introduced. The Figure 3.2., shows some selected stations from gathered information. Actually there are plenty of control points because of the mapping activities all around the region. The points shown in the Figure 3.2., are some of the suitable locations according to the fault trace. Moreover, there is still

need to interpret a final solution for the station locations from the elements of the whole geodetic control point set. The final geometry is going to be expressed in terms of above algorithms and parameters.

Figure 3.2. Locations of some control stations

3.2. Network Design

Global Positioning System became a powerful geodetic tool, while it was designed for the military purposes by the US Department of Defense. The motion of the tectonic plates, deformation studies around active faults and volcanoes and engineering studies can be determined using GPS measurements. Moreover, with the combination of GPS and tide gauges it is possible to monitor the global sea level changes. Besides, GPS signals are measurably delayed as they pass through the earth's atmosphere; and it is also possible to contribute to atmospheric studies with GPS measurements (Segall, Davis, 1997). GPS provides three-dimensional relative position information over base line separations of hundreds of meter to thousands of kilometers with the precision of a few millimeters to

approximately one centimeter. Different from the conventional geodetic techniques, (horizontal and vertical measurements) GPS enables three-dimensional position information and one can determine the vertical as well as horizontal displacements at the same time. Besides, GPS has a lot of advantages such as the portable receivers and antennas, operational under all atmospheric conditions and not requiring visibility between the geodetic control stations. Unlike the other space geodetic techniques, such as Very Long Baseline Interferometry (VLBI) and Satellite Laser Ranging (SLR) which require large facilities and budgets, GPS became an inexpensive and precise geodetic tool in crustal deformation research. GPS has already had a significant impact on earth sciences, and lots of scientific researches performed using GPS technique. The following chapter is going to explain the basics briefly.

The contribution of GPS to the deformation studies can be defined as co-seismic, post-seismic and inter-seismic deformations. Co-seismic displacements have been determined with GPS for almost two decades, including the 1999 Izmit Earthquake (Figure 3.3.). GPS measurements of surface displacement determine the rapture geometry of the earthquakes. Some earthquakes do not rapture the ground surface or in some cases seismic data would not be able to determine the rapture geometry. For this reason, GPS measurements become dramatically important in determining such parameters. The fault geometry is important because of the necessity to determine the distribution of slip on the fault surface and some optimization processes have to be performed in order to estimate source geometry from observed displacements.

Although the information about source geometry can be obtained from the seismic data and direct observations from the fault rapture, in some cases non-geodetic techniques mentioned above are insufficient. There are some conditions that seismic and geological data often do not completely constrain the fault geometry. In some cases, primary fault rapture does not reach the earth surface. Besides, aftershock distributions can be complex, so the geodetic observations would play a substantial role in defining the geometry of the fault trace.

Post-seismic interval generally includes considerable information about the possible earthquakes, and the data collected by GPS improves the knowledge of these post-seismic activities. Conventional seismic instrumentations are very intensive to post-seismic processes except defining the aftershocks (Segall, Davis, 1999). The spatial coverage and the long-term stability of the geodetic survey measurements make it possible to resolve the post-seismic strains with characteristic times of years to decades; however, strainmeters and tiltmeters are able to record short-term transients following earthquakes. Moreover, it is certain that continuously operating GPS stations and dense networks enable researches to investigate post-seismic terms in detail on upcoming decades. In other words, geodesists will able to resolve rapid post-seismic signals that were only measurable with strain and tilt meters before, by the proliferation of continuous GPS stations.

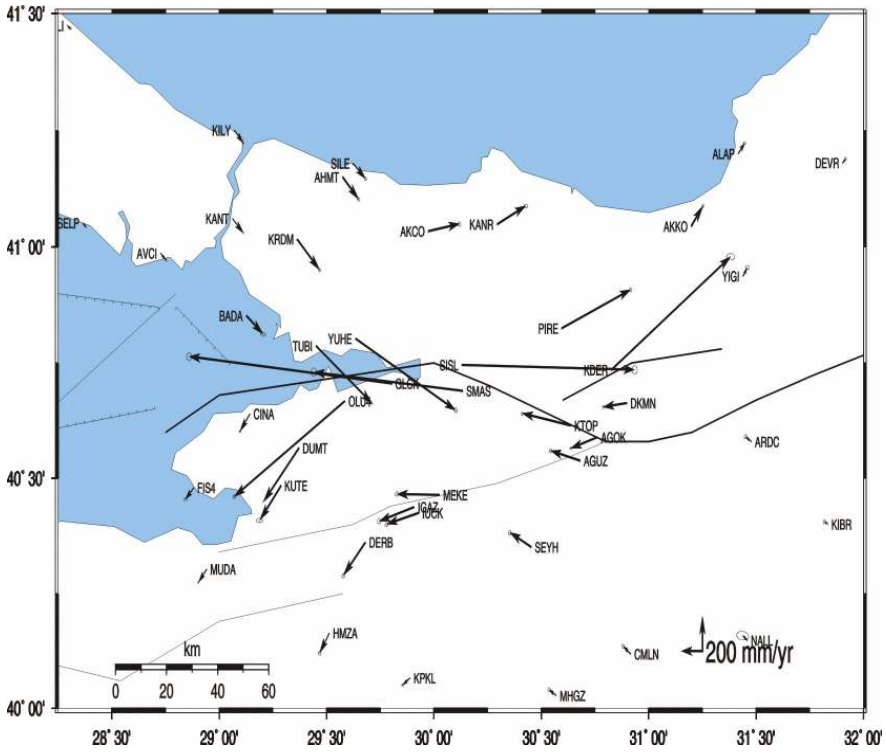

Figure 3.3. Co-seismic displacement after 1999 Izmit Earthquake (Ozener H., 2000)

Observations show that, deformation rates along plate boundaries are considerably higher than those in intraplates and GPS technique provides valuable information about the intraplate deformation. Remeasuring existing geodetic networks by GPS is a powerful strategy for obtaining strain estimates without waiting for long periods of time. Moreover, today a world wide continuously operating reference stations network (Figure 3.4.) provide high precision four dimensional data for geodetic stations make considerable contribution to geodynamics.

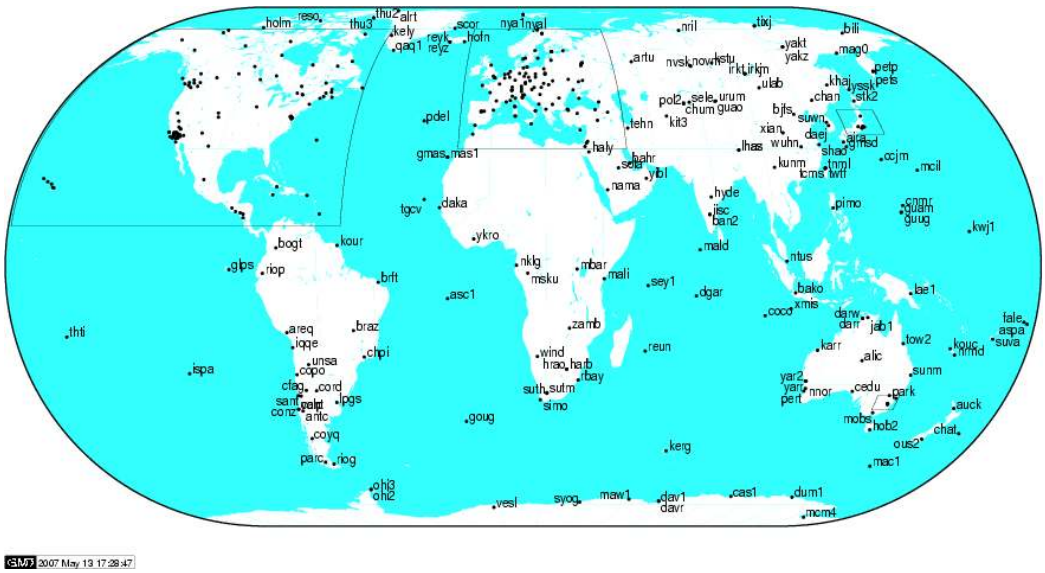

Figure 3.4. ITRF2000 Network

Especially for last two decade in the area of studies for crustal deformation along plate boundaries and individual fault traces is grown so the interest on an optimal design of monitoring schemes increased. Because of the effectiveness of the GPS on crustal deformation monitoring processes the optimal design of monitoring network becomes a great practical interest. Designing a geodetic network can be generally divided into four main stages.

The Zero-Order Design (ZOD) which generally deals with the definition of the optimum reference system of the network.

The First-Order Design (FOD) involves the geometric shape of the network including the optimum number and locations of the geodetic stations.

On the other hand the Second-Order Design (SOD) deals with the determination of the weights of network measurements. SOD interested in which observations and with what precision should be achieved in the network.

Finally the Third-order Design (TOD) considers the improvement of an existing network including the additional measurements that has to be made with the desired precision and what weights are selected for the improvement of network. Schmitt 1982 claim that in case the period of time between consecutive observations taken into account the term fourth order design maybe used.

The main purpose of the optimization on a geodetic network is related with the design geodetic survey to achieve the desired level of accuracy, reliability and low cost (Gerasimenko, *et al.,* 2000). On the other hand there is no systematic and formulated solution about the number of stations that the network should include although there are some approaches on that topic (Gerasimenko, *et al.,* 2000, Blewitt, 2000, Shestakov *et al.,* 2003). Moreover there is a lack of information about the locations of the stations in order to collect more information about the mechanics or deformations over active faults.

In order to define the number of station that should be added into a deformation network or which sites should be used for that purpose is directly concerned with the phenomenon understanding fault mechanics. Gerasimenko *et al.,* (2000) conformed a model for this purpose by using simple strike-slip fault model in which the deformations are parallel to the fault trace, in order to facilitate the problem. A one-dimensional fault

model with two parameters standard strike-slip model of dislocation theory in an elastic half-space can be formulated as;

$$d(x) = -\frac{V}{\pi}\arctan\left(\frac{x}{H}\right) \tag{3.1}$$

Where x is the distance perpendicular to the fault, and the fault plane extends from the surface of the half space to infinite depth, locked from the surface to H km, and freely slipping below this depth V millimeter per year.

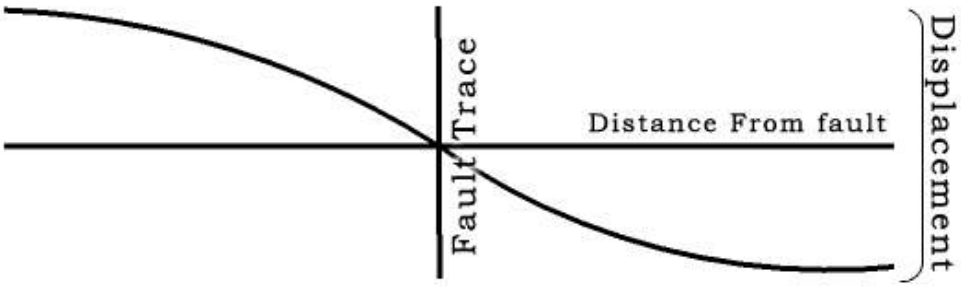

Figure 3.5. Expected surface deformation as a function of distance from the fault trace

For a right-lateral motion the uniform motion of two blocks relative to a fixed reference frame is positive. The expected surface deformation can be shown as in Figure 3.5. as a function of distance from the fault trace.

One model that is going to be introduced briefly here is a one dimensional two parameter standard strike slip model of dislocation theory. It is assumed that the fault is long and straight, and in the direction of fault strike the deformation produced is uniform. This kind of model is suitable for San Andreas, North Anatolian Fault systems. It is that the parallel displacements from the fault trace *d(x)* can be expressed with a standard deviation of m_d. The standard deviation m_d includes the monument instability and some

other types of errors. Considering these errors and eliminating them is important because of the effect they produce on tectonic signals which is directly effect the interpretations.

In the deformation monitoring networks, the economy as function, should be considered and the network should be developed and observed using the most economical way and should satisfy a desired precision and reliability criteria set by the user. In dense GPS network, and especially the ones that are designed for campaign based observations has many control stations and field measurements have a significant contribution to the campaign cost. Therefore one can easily realize that the most important criterion to the network is the campaign cost requirement. There is a common criterion for optimization can be stated as;

$$\Phi = \sum_{1}^{n} c_i p_i \rightarrow \min \tag{3.2}$$

$$p_i = \left(\frac{1}{m_{d_i}^2} \quad or \quad 0 \right) \tag{3.3}$$

where p_i is the weight of the observations and c_i is the chosen coefficient of the profitableness for observable. The coefficient $c_{i,}$ is taken in to account when erecting the monument, transportation to the station and other costs. If the p_i is equal to zero, it means that the corresponding observables do not contribute the accuracy of fault parameters to be investigated. Therefore the observables should be deleted from the final observation scheme. The weight of the observations p_i can be written as follows to facilitate the problem

$$0 \leq p_i \leq p_{i,\max} \tag{3.4}$$

$$p_{i,\max} = \frac{1}{m_{d_i}^2} \tag{3.5}$$

The weight, $p_{i,max}$ is the maximum accessible weight. The constraint equation of $p_{i,max}$ states that the weights should be optimally solved for and should be non-negative and achievable with the given instrumentation (Gerasimenko, *et al.,* 2000). It is certain that optimization allow choosing the following function instead of target function Φ,

$$\Phi_1 = \sum_1^n c_i p_i \rightarrow \max \tag{3.6}$$

Φ_1 is the optimum maximum and Φ is the optimum minimum function so, those two parameters are not equivalent to each other the in mathematical sense . When individual weight $p_i \rightarrow 0$, the function $\Phi_1 \rightarrow \infty$ so the numerical problem of solving occurs.

The other criteria of the monitoring network are the precision requirements. It can be expressed as constraint equations for the precision of the slip rate and locking depth

$$m_V^2 \le m_{V,\max}^2 \; and \; m_H^2 \le m_{H,\max}^2 \tag{3.7}$$

Above inequality expressions are applied to ensure that the resulting accuracies m_V and m_H of the parameters V and H are better or equal to a certain boundary values accuracy $m_{V,max}$ and $m_{H,max}$. The covariance matrix can be stated as

$$Q = \begin{pmatrix} Q_{VV} & Q_{VH} \\ Q_{HV} & Q_{HH} \end{pmatrix} = \begin{pmatrix} \sum p_i a_i a_i & \sum p_i a_i b_i \\ \sum p_i a_i b_i & \sum p_i b_i b_i \end{pmatrix}^{-1} \tag{3.8}$$

And the values $m_V^2 = Q_{VV}$ and $m_H^2 = Q_{HH}$ are the diagonal elements of the covariance matrix. The coefficients a_i and b_i comes from the linearization of the model equation (3.1) as,

$$\delta d(x_i) = a_i \delta V + b_i \delta H \tag{3.9}$$

where

$$a_i = \frac{\delta d(x_i)}{\delta V} = -\frac{1}{\pi} arctg\left(\frac{x_i}{H}\right) \tag{3.10}$$

$$b_i = \frac{\delta d(x_i)}{\delta H} = \frac{V}{\pi} \frac{x_i}{H^2 + x_i^2} \tag{3.11}$$

It is certain that more complicated model of the fault can be taken into consideration than the two parameter model, incorporates the reliability and the total number of redundant observables in order to obtain a multi-objective optimal design.

These equations formed in order to estimate the fault-model parameters, slip rate and locking depth and define a practical method for the optimal design of geodetic monitoring schemes. According to Gerasimenko *et al.,* (2000), the smaller is a slip-rate the more points must be included to the network especially a nearby fault as well.

Besides the determination of position accuracy of the survey network in order to obtain the best measurements some other studies (Taskin *et al.,* 2003) focus on the figuring

out the network design problem. By using the synthetic data, some researches tried to decide where the individual stations should be located in the network, how many stations should be included to a network or which sites should be chosen to optimize for better understanding the fault mechanics. Taskin *et al*., (2003) produce synthetic data by using a computer program.

The one dimensional fault model with two parameters standard strike-slip model of dislocation theory in an elastic half space is formulated as the surface displacement parallel to the fault trace. An ideal geometry selected as the stations are symmetrically distributed in an equal distance from each other to the both sides of the fault.

It was assumed that space geodetic technique is able to determine the fault parallel displacement with a standard deviation of ±1 mm for measurement errors. For whole geodetic stations the monument instability assumed as ±1 mm. the fault model parameters are chosen as 10 km locking depth (*H*) and the slip rate (*V*), 10 mm per year. The number and position of the stations tried to be evaluated by using following results.

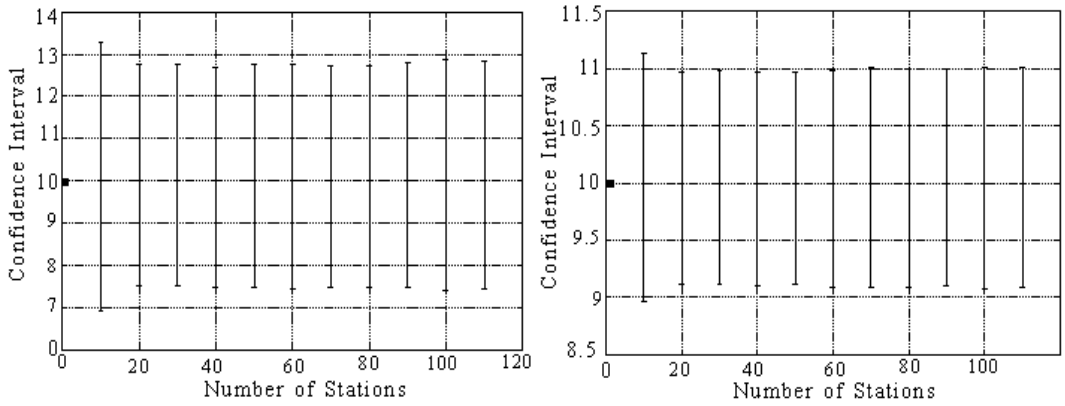

Figure 3.6. Individual confidence limits on the locking depth and slip rate as a number of stations respectively (Taskin *et al.,* 2003)

During the first step of the optimization in the experiment, to define the effect of number of stations in the network the numbers of geodetic stations are increased and some results have drawn in Figure 3.6.

The increase in number of stations tighter the individual confidence limits on both locking depth and slip-rate; however, the gain from this increase is very small and can be neglected. There is a great tightening at about 20 stations but than it stays approximately at about a constant rate. On the other hand, according to the positions of the stations, the sensitivity coefficients of the model parameters *V,* and *H* vary with respect to the distance from the fault (Figure 3.7.).

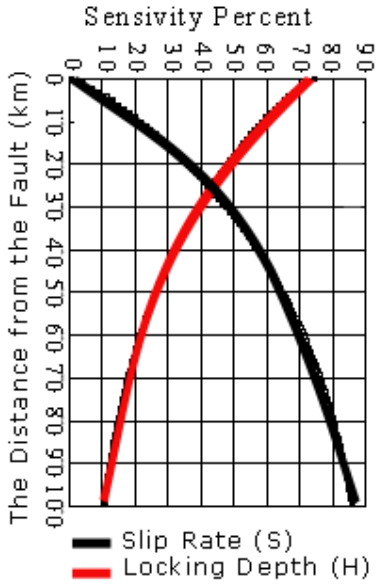

Figure: 3.7. Sensitivity coefficients for slip rate and locking depth with respect to the distance from the fault trace (Taskin *et al.,* 2003)

According to the figures generated, in order to determine the locations of the stations, they should be located near the fault trace if the locking depth *H* is tried to be estimated. Otherwise, if the slip-rate is going to be estimated the station locations should be far from the fault trace.

Blewitt (2000), generalize the first order design problem by suggesting network configurations that optimizes the precision of network parameters. The formulization of the problem can be designed as geodetic and geophysical functional model. Geodetic model includes the station numbers n and positions r_i (where i=1,2,3, ….m). It can be modeled as the geodesy can provide estimates of m station velocities u_i with an m x m covariance matrix C. W is the fully populated weight matrix formed from inverse of C. The station velocity vector u_i can also be written as an analytical function of station position r_i and geophysical parameters g_k as follows;

$$\begin{aligned} u_1 &= G(r_1; g_1, g_2, ...g_n) \\ u_2 &= G(r_2; g_1, g_2, ...g_n) \\ &\vdots \\ u_m &= G(r_m; g_1, g_2, ...g_n) \end{aligned} \tag{3.12}$$

In preparation of weighted least squares analysis, above equation is linearized about provisional parameter values (denoted by lines):

$$u_i = G(r_i; \overline{g}_1, \overline{g}_2, ...\overline{g}_n) + A.(g - \overline{g}) \tag{3.13}$$

Equation (3.13) shows how parameter precision depends on the network design. The mxm A matrix contains the partial derivatives of the velocity model with respect to the geophysical parameters evaluated at the provisional values.

$$A_{ik} = \frac{\partial G(r_i; g_{1,} g_2, ..., g_n)}{\partial g_k}\Bigg|_{\overline{g}_{1,} \overline{g}_2, ..., \overline{g}_n} \tag{3.14}$$

The variances and covariance of the estimated parameters are given in the matrix P which is a function of all station positions and provisional parameters.

$$P(r_1, r_2, ...r_m; \overline{g}_1, \overline{g}_2, ...\overline{g}_n) = (A^T WA)^{-1} \tag{3.15}$$

Matrix *P* characterizes the precision of the parameters. The overall precision is also can be characterized by a single number, which can be minimized by varying the station locations. Then a J matrix which is a function of covariance matrix can be defined as:

$$J\{P(r_1, r_2, ...r_m; \overline{g}_1, \overline{g}_2, ...\overline{g}_n)\} \tag{3.16}$$

The above definition yield a single number of assessment for each network that defined by the set $\{r_i \mid i=1,2....m\}$.if this functional varied by perturbing station positions by $\delta \mathbf{r}_i$,

$$\delta J\{P(r_1, r_2, ...r_m; \overline{g}_1, \overline{g}_2, ...\overline{g}_n)\} = \frac{\delta J}{\delta \mathbf{r}_1}\delta \mathbf{r}_1 + \frac{\delta J}{\delta \mathbf{r}_2}\delta \mathbf{r}_2 + \ldots + \frac{\delta J}{\delta \mathbf{r}_m}\delta \mathbf{r}_m \tag{3.17}$$

If the variation is zero for any set of station perturbations, the set of station positions $\mathbf{r}_i$`minimize this function. For every station *I,*

$$K_i(r_1', r_2', ...r_m'; \overline{g}_1, \overline{g}_2, ...\overline{g}_n)\} = \frac{\delta J}{\delta \mathbf{r}_i} = 0 \tag{3.18}$$

The problem of generalized first order design is stated as finding the that satisfies above equation set of $\mathbf{r}_i$` ($i=1,2,...m$), for a specific functional $J$. Therefore, the system can be defined as a system of $m$ equation, each station has different vector function $K_i$, and $m$, and unknown positions ($r_{1`}$,$r_{2`}$,…$r_{m`}$) which are going to be solved.

Blewitt (2000), offers a new analytical method, generalized first order design is proposed for optimizing geodetic station locations for purposes of geophysical parameter estimation. The method given by the equation (3.19), finds the set of station locations that maximizes the determinant of the design matrix.

$$\frac{\partial}{\partial r_i} \det A = 0 \tag{3.19}$$

The method that Blewitt (2000) suggests, leads to exact analytical solutions for the ideal transform fault locked down to depth D. According to this method, to resolve the depth of locking D and the location of the fault simultaneously, optimal station locations are at $\pm D\sqrt{3}$ from the a priori fault plane. On the other hand, analysis of slip partitioning in two-fault system shows that the resolution is optimized by including a station between faults. If the distance between faults is greater than $2D$ which is approximately 30 km the resolution is limited.

3.3 Izmir Microgeodetic Network

According to the optimization strategies, performed experiments and collected information stated above, a geodetic network had designed and interpretation strategies are discussed in order to monitor Tuzla fault and its vicinity.

Network designed on the information of existing control points and the fault trace geometry. Some additional stations were established in order to define the locking depth and slip rate of the fault trace according to the conclusions defined above subtitles. Moreover, because of the possibility of the extension of the study area, other active fault had taken into consideration in design process. The station names are reorganized accordingly except the TNFGN stations with four character letters.

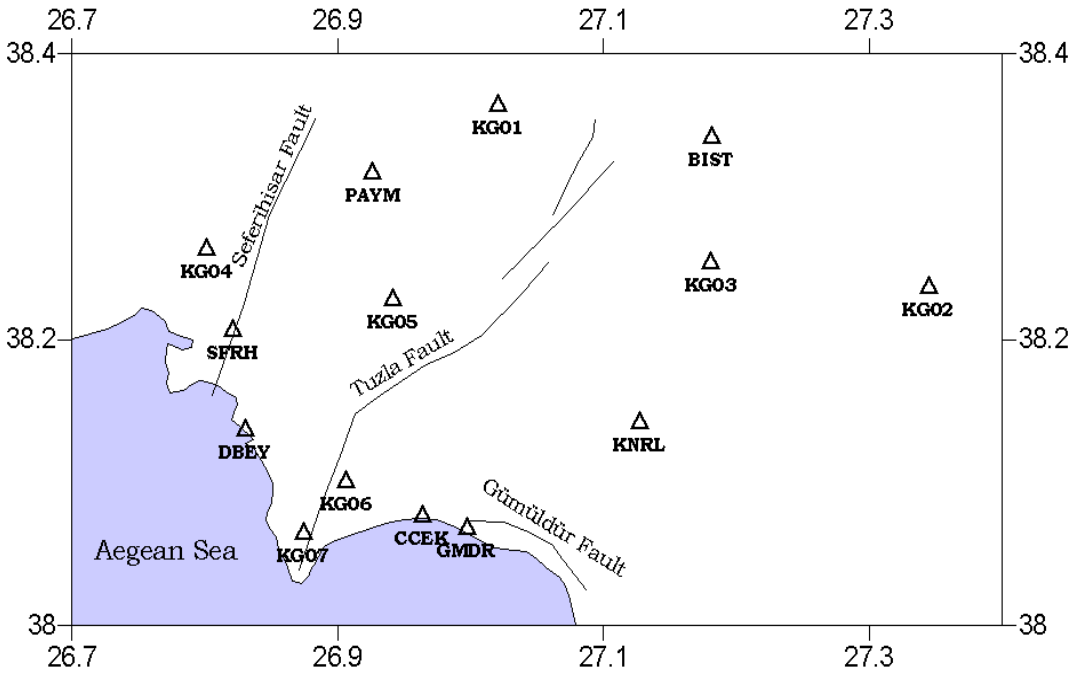

Figure 3.8. Locations of the sites of Izmir microgeodetic network

After the discussions to the local administrations 14 control stations were selected for the network from hundreds of sites. There are lots of station points established through the region especially in last 3 years for cadastre projects.

Figure 3.8. shows the locations of the sites and approximate trace of Tuzla fault and Seferihisar fault. Stations are distributed both on the fault trace and far from the fault at about 20 km. The stations are close to each other along the south segment of Tuzla fault

because the fault has a very complex and sectional structure on the south (Figure 2.10.). There are some short baselines in the network such as CCEK-GMDR baseline because of the adjacency of two active faults. There is another fault very near to Tuzla fault and GMDR and CCEK points are very close to that Gumuldur fault. The WGS84 coordinates of the control station shown in Table 3.1.

Table 3.1. Locations of network stations

Site name	φ Latitude (in Degrees)	λ Longitude (in Degrees)
KG01	38,36416	27,02072
KG02	38,23637	27,34451
KG03	38,25372	27,18084
KG04	38,26320	26,80143
KG05	38,22815	26,94152
KG06	38,10099	26,90646
KG07	38,06433	26,87388
PAYM	38,31700	26,92600
KNRL	38,14244	27,12700
GMDR	38,06800	26,99700
DBEY	38,13700	26,83000
SFRH	38,20700	26,82100
BIST	38,34200	27,18100
CCEK	38,07659	26,96351

In conclusion, the locations of the stations points of microgeodetic network distributed to the both side of the fault. Moreover, some stations are located very near to the fault trace and some others far from the fault trace at about 20 km, according to the distribution of the surface deformation with respect to the distance from the fault trace.

The network is compatible to the studies performed in first order network design studies. Generally the line connecting GPS stations are in align with the direction of extension or compression, the angles of triangles composed by GPS stations are generally between 30 and 130 degrees (Wu *et al.,* 2003). On the other hand, some additional points that had added to the network like GMDR, KG07, KG06, and KG02 do not satisfy the above rules. However, those points are selected consciously because the southern segment

of the faults has a very complex structure and composed of several pieces. KG02 is selected because the results wanted to be evaluated in terms of short and long baselines and for various perpendicular distances to the fault trace.

Moreover, a block exists in the middle of Karaburun peninsula has a differential motion at a rate of 3–5±1 mm/year to the east and 5–6±1 mm/year to the south (Aktug and Kilicoglu, 2006). Therefore, 14 points thought to be enough for determining the slip rate which is not as small as stated in Gerasimenko (2000). The network designed to be suitable for future studies which have a possibility to enlarge the project area, so the suggestions mentioned in Blewitt (2000) are taken into consideration. The sites are also selected according to the transportation possibilities and visibility of open sky. The reconnaissance performed in the region made it easy to define those site proporties. Some photographs of the sites are shown in following Figures 3.9., 3.10. and 3.11.

Figure 3.9. CCEK, looking to the south

Figure 3.10. SFRH, looking to the north

Figure 3.11. Investigation of field team on Tuzla fault for station locations.

4. DATA ANALYSING STRATEGIES

4.1 The Theory of GPS Processing

First of all, it is thought to be necessary to state the theoretical background of the technique that is going to be used during the study. GPS technique which is based on the triangulation technique in defining the coordinates of the receiver location from the location of the satellites at an epoch *t* uses two main determination techniques. First technique is defined as the Pseudorange Observation Equations and the second technique is the Carrier Phase Observable. The theoretical background of the Pseudorange Observation Equations can be stated as follows;

During an observation receivers record the data at specified intervals for example at every 15 seconds. When the measurement is sampled the receiver clock time *T* is recorded. In other words, the value of receiver clock time *T*, at a measurement epoch is known exactly, and is written to the data file along the observation but the unknown is the true time of measurement. The actual observation to satellite *s* can be written as;

$$P^s = (T - T^s)c \tag{4.1}$$

where T is the known reading of the receiver clock when the signal is received, T^s is the reading of satellite clock when signal was transmitted, and c is the speed of light (c=299792458 m/s). Figure 4.1. shows a schematic diagram of the relationships between these values.

It is possible to set an equation between the true clock time *T,* and true receiver time *t* by a clock bias τ, for both receiver and satellite clocks. Then it is possible to substitute the above equations to the pseudorange which is a function of true time

$$T = t + \tau \tag{4.2}$$

$$T^s = t^s + \tau^s \tag{4.3}$$

$$P^s(t) = ((t+\tau) - (t^s + \tau^s))c = (t - t^s)c + c\tau - c\tau^s = \rho(t, t^s) + c\tau - c\tau^s \tag{4.4}$$

where $\rho(t\text{-}t^s)$ is the range from receiver at receive time to the satellite at transmit time. The model can be simplified as using the Pythagoras Theorem like;

$$\rho^s(t, t^s) = \sqrt{(x^s(t^s) - x(t))^2 + (y^s(t^s) - y(t))^2 + (z^s(t^s) - z(t))^2} \tag{4.5}$$

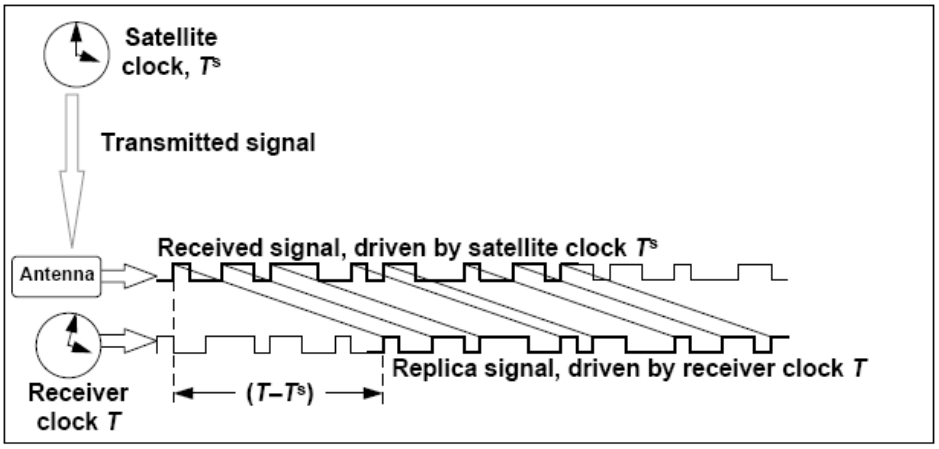

Figure 4.1. The relation between GPS Pseudorange observations, and satellite and receiver

It is possible to compute the satellite position (x^s, y^s, z^s) and the satellite clock bias τ^s, by using the Navigation massage. Therefore, there are 4 unknowns in the problem, the

receiver coordinates *(x,y,z)* and the receiver clock bias τ. On the other hand, satellite position must be calculated at transmission time, t^s; however, there is a change in satellite's position between the time transmission time and the receive time of the signal. In order to figure out this problem starting with the receive time, *t*, the transmit time can be computed by using an iterative algorithm known as the light time equation. By using this iterative method satellite position hence the pseudorange is calculated at each step using the Keplerian-type elements from the Navigation massage until it converges to a negligible difference.

Finally the 4 pseudoranges to each satellite can be written as (the superscripts indicates the satellite numbers);

$$\begin{aligned} P^1 &= ((x^1 - x)^2 + (y^1 - y)^2 + (z^1 - z)^2)^{1/2} + c\tau - c\tau^1 \\ P^2 &= ((x^2 - x)^2 + (y^2 - y)^2 + (z^2 - z)^2)^{1/2} + c\tau - c\tau^2 \\ P^3 &= ((x^3 - x)^2 + (y^3 - y)^2 + (z^1 - z)^3)^{1/2} + c\tau - c\tau^3 \\ P^4 &= ((x^4 - x)^2 + (y^4 - y)^2 + (z^4 - z)^2)^{1/2} + c\tau - c\tau^4 \end{aligned} \tag{4.6}$$

Using the least squares methods it is possible to solve the equations with 4 unknowns, *(x,y,z,τ)*, although it not necessary for 4 unknowns with 4 parameters but if the case of more than 4 satellites is considered in view the solution can be generalized. Using the methods of least-squares analysis, the GPS point positioning problem can be solved by linearising the pseudorange observation equations.

$$P_{observed} = P_{model} + noise \tag{4.7}$$

$$P_{observed} = P(x,y,z,\tau) + v \tag{4.8}$$

Actual observations can be assumed to be written as sum of the model observations and an error term. Then model computing can be expanded using the provisional parameter

values (x_0,y_0,z_o,τ_0), Taylor's theorem can be applied. Final expression can be written as in matrix form by ignoring second and higher order terms of Taylor's theorem.

$$\Delta P = \begin{pmatrix} \frac{\partial P}{\partial x} & \frac{\partial P}{\partial y} & \frac{\partial P}{\partial z} & \frac{\partial P}{\partial \tau} \end{pmatrix} \begin{pmatrix} \Delta x \\ \Delta y \\ \Delta z \\ \Delta \tau \end{pmatrix} + v \tag{4.9}$$

In general for m satellites in view the above expression can be written as;

$$\begin{pmatrix} \Delta P^1 \\ \Delta P^2 \\ \Delta P^3 \\ \vdots \\ \Delta P^m \end{pmatrix} = \begin{pmatrix} \frac{\partial P^1}{\partial x} & \frac{\partial P^1}{\partial y} & \frac{\partial P^1}{\partial z} & \frac{\partial P^1}{\partial \tau} \\ \frac{\partial P^2}{\partial x} & \frac{\partial P^2}{\partial y} & \frac{\partial P^2}{\partial z} & \frac{\partial P^2}{\partial \tau} \\ \frac{\partial P^3}{\partial x} & \frac{\partial P^3}{\partial y} & \frac{\partial P^3}{\partial z} & \frac{\partial P^3}{\partial \tau} \\ \vdots & \vdots & \vdots & \vdots \\ \frac{\partial P^m}{\partial x} & \frac{\partial P^m}{\partial y} & \frac{\partial P^m}{\partial z} & \frac{\partial P^m}{\partial \tau} \end{pmatrix} \begin{pmatrix} \Delta x \\ \Delta y \\ \Delta z \\ \Delta \tau \end{pmatrix} + \begin{pmatrix} v^1 \\ v^2 \\ v^3 \\ \vdots \end{pmatrix} \tag{4.10}$$

with matrix symbols;

$$\mathbf{b=Ax+v} \tag{4.11}$$

Above matrix expression indicates a linear relationship between the residual observations **b** (observed minus computed observations) and the unknown correction parameters **x**. The column matrix **v** contains all noise terms and above equation is called as "linearized observation equations".

The design matrix, **A**, contains the linear coefficients, which are the partial derivatives of each observation to the each parameter and computed using the provisional parameters values.

$$A = \begin{pmatrix} \frac{x_0 - x^1}{\rho} & \frac{y_0 - y^1}{\rho} & \frac{z_0 - z^1}{\rho} & c \\ \frac{x_0 - x^2}{\rho} & \frac{y_0 - y^2}{\rho} & \frac{z_0 - z^2}{\rho} & c \\ \frac{x_0 - x^3}{\rho} & \frac{y_0 - y^3}{\rho} & \frac{z_0 - z^3}{\rho} & c \\ \vdots & \vdots & \vdots & \vdots \\ \frac{x_0 - x^m}{\rho} & \frac{y_0 - y^m}{\rho} & \frac{z_0 - z^m}{\rho} & c \end{pmatrix} \tag{4.12}$$

It is obvious that above design matrix, **A**, is a function of the direction to each of the satellites as observed from the receiver. Considering $\hat{\mathbf{x}}$, for the solution of linearised observation equations then the estimated residuals are defined as the difference between the actual observations and the estimated model for the observations.

$$\hat{\mathbf{v}}=\mathbf{b}-\mathbf{A}\hat{\mathbf{x}} \tag{4.13}$$

The solution of normal equations will be;

$$\mathbf{x}=(\mathbf{A}^T\mathbf{A})^{-1}\mathbf{A}^T\mathbf{b} \tag{4.14}$$

On the other hand, any errors on **v** in the original observations **b** will map into errors $\mathbf{v}_x$ in the estimates of $\hat{\mathbf{x}}$.

$$\mathbf{v_x}=(\mathbf{A^T A})^{-1}\mathbf{A^T v} \tag{4.15}$$

If the expected value for the error in the data, σ, is assumed then it is possible to compute the expected error in the parameters. Under the assumptions of characterizing the error in the observations with one number, the variance $\sigma^2=E(v^2)$ and all observations are uncorrelated, $E(v_i v_j)=0$ (for i≠j) the least squares solution can be written as in a simple form;

$$\mathbf{C_x}=\boldsymbol{\sigma}^2\times(\mathbf{A^T A})^{-1} \tag{4.16}$$

Cofactor matrix $\mathbf{(A^T A)^{-1}}$ also in the formula of the least squares estimate, $\hat{\mathbf{x}}$. GPS observation errors are a strong function of particular situation and it is common to focus on covariance matrix, which like **A**, is purely a function of the satellite-receiver geometry at the times of the observations. The cofactor matrix can therefore be used to assess the relative strength of the observing geometry, and to quantify how the level of errors in the measurements can be related to the expected level of errors in the position estimates. Therefore, it is possible to compute the cofactor matrix in advance of surveying session using the almanac in Navigation Massage (for the satellite positions) by using the "Design Matrix" **A**. finally one can design his survey poor satellite geometry will not limit the position precision. In order to discuss the correlation between parameters, the covariance matrix of the estimated parameters has to written in terms of its components.

$$C_x = \sigma^2 \begin{pmatrix} \sigma_x^2 & \sigma_{xy} & \sigma_{xz} & \sigma_{x\tau} \\ \sigma_{yx} & \sigma_y^2 & \sigma_{yz} & \sigma_{x\tau} \\ \sigma_{zx} & \sigma_{zy} & \sigma_z^2 & \sigma_{z\tau} \\ \sigma_{\tau x} & \sigma_{\tau y} & \sigma_{\tau y} & \sigma_\tau^2 \end{pmatrix} \tag{4.17}$$

The off-diagonal elements indicate the correlation between parameters. Correlation coefficient can be written as follows in order to define measure of correlation;

$$\rho = \frac{\sigma_{ij}}{\sqrt{\sigma_i^2 \sigma_j^2}} \tag{4.18}$$

The correlation coefficient is only a function of cofactor matrix and is independent from the observation variance, σ^2. When focusing on the horizontal and vertical positions of the station in applications one should consider the vertical component of the position tends to have a larger error than horizontal coordinates. For this reason it is convenient to use local geodetic coordinates, therefore a transformation is necessary from geocentric coordinates *(u,v,w)* to local topocentric coordinates *(n,e,h)*. The covariance matrix also has to be transformed according to the law of error propagation. *G* is the transformation matrix; φ and λ are latitude and longitude respectively.

$$\mathbf{\Delta L = G \Delta X} \tag{4.19}$$

$$\begin{pmatrix} \Delta n \\ \Delta e \\ \Delta h \end{pmatrix} = \begin{pmatrix} -\sin\varphi\cos\lambda & -\sin\varphi\sin\lambda & \cos\varphi \\ -\sin\lambda & \cos\lambda & 0 \\ \cos\varphi\cos\lambda & \cos\varphi\sin\lambda & \sin\varphi \end{pmatrix} \begin{pmatrix} \Delta x \\ \Delta y \\ \Delta z \end{pmatrix} \tag{4.20}$$

It is certain that **G** matrix also transforms the errors in **ΔX** into errors **ΔL** which can be expressed as $\mathbf{v_L = G v_X}$. According to law of propagation of errors, the transformation of covariance matrix of coordinates from geocentric system to the local system can be written as follows:

$$\mathbf{C_L = G C_X G^T} \tag{4.21}$$

$$C_L = \sigma^2 \begin{pmatrix} \sigma_n^2 & \sigma_{ne} & \sigma_{nh} \\ \sigma_{en} & \sigma_e^2 & \sigma_{eh} \\ \sigma_{hn} & \sigma_{he} & \sigma_h^2 \end{pmatrix} \tag{4.22}$$

Above equation can be applied to any problem involving an affine transformation. This covariance can be also used to plot error ellipses in the horizontal plane.

Various types of dilution of precision (DOP) values can be defined as a function of the diagonal elements of the covariance matrix in local system.

$$\begin{aligned} VDOP &= \sigma_h \\ HDOP &= \sqrt{\sigma_n^2 + \sigma_e^2} \\ PDOP &= \sqrt{\sigma_n^2 + \sigma_e^2 + \sigma_h^2} \\ TDOP &= \sigma_\tau \\ GDOP &= \sqrt{\sigma_n^2 + \sigma_e^2 + \sigma_h^2 + c\sigma_\tau^2} \end{aligned} \tag{4.23}$$

VDOP stands for the vertical dilution of precision, H stands for the horizontal, P for precision, T for time, and G for geometric. Finally, it can be evaluated as the *DOP* values are purely as a function of satellite geometry as observed by the receiver and low *DOP* values point good satellite geometry where high values means bad satellite geometry. In practice, generally *PDOP* values larger than 5 considered as poor.

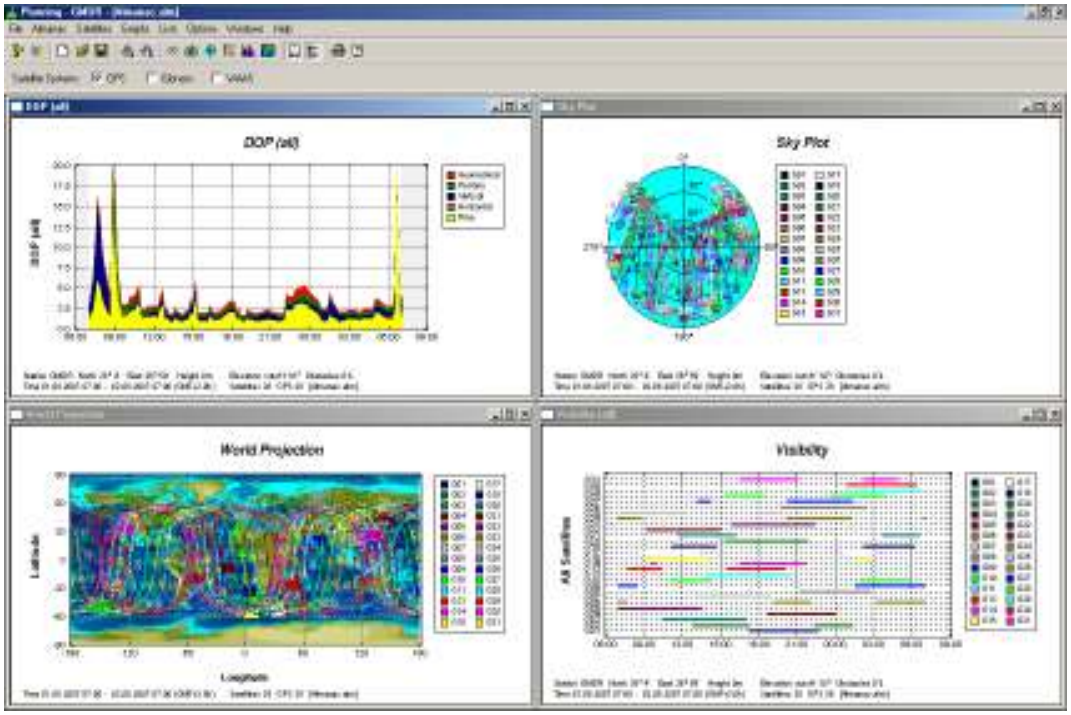

Figure 4.2. Sky plots and DOP values produced with Trimble Geomatics Office for GMDR station

Consequently, pre-analyzing of satellite geometry has a dramatic importance before the field observations which is described as mission planning. Generally in the market, commercial GPS processing software can be used to plot DOP values between given time interval and given location. Figure 4.2. shows DOP values and sky plots for GMDR station (38^0 4' N, 26^0 59'E) of Izmir Microgeodetic Network at 1^{st} of August, 2007 with an elevation mask 10 degrees, beginning from 7 pm using the satellite almanac data. Additional information is also available for wide information in interpretation such as including GLONASS and WAAS systems' satellite consolidation data. If the condition of the station s known then some specific information also can be added like trees, or building to the obstacles menu and re-evaluating the results for mission planning would be more precise. Mission planning stage of the observation preparation is important in designing the surveying interval and observation time. This stage of design is going to be detailed in latter topics.

Carrier Phase observable is more accurate in positioning than pseudorange and therefore used for high precision applications. It is possible to describe the process of observing the carrier phase, and develop an observation model. Above formulations for pseudorange observable can be reduced to the process of observing carrier phase. Blewitt (1997) developed an approach of presenting the model in the "range formulism", where the carrier phase expressed in units of meters rather than cycles. However, there are some fundamental differences between the carrier phase and pseudorange observables.

Some of the following paragraphs are going to give some brief definitions about some fundamental expressions such as Phase, Frequency and Clock Time.

Phase is basically the angle of rotation which is in units of cycles for GPS analysis. If a point is considered moving counter-clockwise around the edge of a circle, then a line is drawn from the centre of the circle to the point, the phase $\varphi(t)$, at any given time t can be defined as the angle through which this line has rotated.

Phase is intimately connected with the concept of time, which is always based on some form of periodic motion, such as the rotation of the Earth, the orbit of the Earth around Sun (dynamic time), or the oscillation of a quartz crystal in a wristwatch (atomic time). Therefore, phase can be thought of as a measure of time after conversion into appropriate units (Figure 4.3.).

The frequency, which is expressed in units of cycles per second, is the number of times that the line completes a full 360^0 rotation in one second. More valuable definition can be, the first derivative of phase with respect to time; that is, the angular speed, $f \equiv d\varphi(t)/dt$.

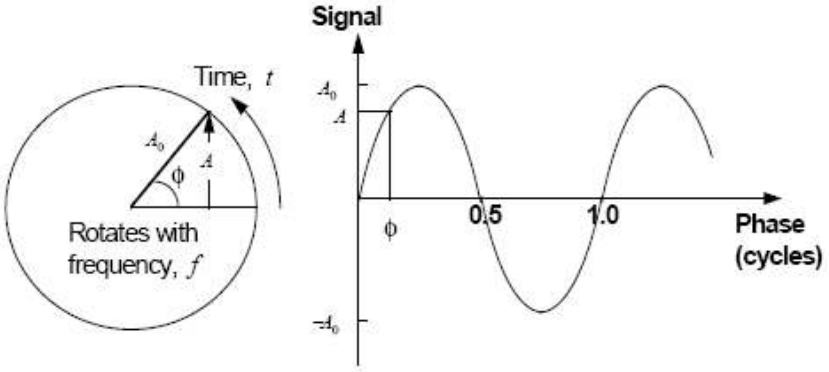

Figure 4.3. The meaning of phase

The GPS carrier signal from the satellite is mixed (multiplied) with the receiver's own replica carrier signal. The carrier phase signal $\varphi_B(t)$ can be defined as the difference in phase between the replica signal and the GPS signal. Moreover, by differentiating this equation with respect to time, the beat frequency can be expressed as the difference between two input signals.

$$\varphi_B(t) \equiv \varphi_R(t) - \varphi_G(t) \tag{4.24}$$

$$f_B \equiv \frac{d\varphi_B}{dt} = f_R - f_G \tag{4.25}$$

In order to produce exactly the same observed beat signal, an integer number of cycles should be added to the beat carrier phase because it not possible to have direct measure of the total phase of incoming GPS signal. This can be expressed by;

$$\Phi + N = \varphi_R + \varphi_G \tag{4.26}$$

Φ emphasizes the phase value actually recorded by the receiver. The receiver track of, how many complete number signal oscillations there have been, since the first measurement. The receiver can attach this number of cycles to the integer portion of the recorded beat phase but there are still be an overall ambiguity *N* that applies to all measurements. Therefore *N*, can be modeled as being the same constant (unknown) for all measurements. If the receiver looses the count of the oscillations then a new integer parameter must be introduced to the model, starting at that time. This integer discontinuity in phase data is called a cycle-slip.

To sum up, the satellite carrier signal from antenna is mixed with the signal generated by the receiver's clock. The result, after a high pass filtering, is a beating signal. The phase of this beating signal equals the reference phase minus the incoming GPS carrier phase from a satellite, but it is ambitious by an integer number of cycles. Observation of satellite S produces the carrier phase observable Φ^S, where φ is the replica phase generated by the receiver clock. φ^S is the incoming signal phase received from GPS satellite *S*, and the measurement is made when the receiver clock time is *T*:

$$\Phi_S(T) = \varphi(T) - \varphi^S(T) - N \tag{4.27}$$

The carrier phase observable $\Phi_A^j(T_A)$, considering the clock time as a function of phase and nominal frequency and substituting all the phase terms with clock times can be written as follows:

$$\Phi_A^j(T_A) = f_0(T_A - T^j) + \varphi_{0A} - \varphi_0^j - N_A^j \tag{4.28}$$

Data should be sampled at exactly the same values of clock time (epochs) for all receivers, so all values of T_A are identical at a given epoch. On the other hand, it is

convenient to convert the carrier phase model into units of range. In the range formulation, carrier phase equation multiplied by the nominal wavelength.

$$\begin{aligned} L_A^j(T_A) &= \lambda_0 \Phi_A^j(T_A) \\ &= \lambda_0 f_0 (T_A - T^j) + \lambda_0 (\varphi_{0A} - \varphi_0^j - N_A^j) \\ &= c(T_A - T^j) + \lambda_0 (\varphi_{0A} - \varphi_0^j - N_A^j) \\ &= c(T_A - T^j) + B_A^j \end{aligned} \tag{4.29}$$

$L_A^j(T_A)$ is the observed range (carrier phase in units of meters), c is the speed of light in vacuum, λ_0 is the nominal wavelength of the signal, B_A^j is the carrier phase bias.

4.1.1. Differencing Techniques

Differencing techniques can be classified as Single Differencing, Double Differencing and Triple Differencing. The aim of single differencing is to eliminate the satellite clock bias. The single Differencing technique has an advantage to eliminate or reduce many error sources, this disadvantage is that only relative position can be estimated (unless the network is global-scale) however, the receiver clock bias is unknown in Single Differencing.

Double differencing (Figure 4.4.) aims to eliminate the satellite clock bias. Single differenced observation equations for two receivers A and B observing satellites j and k can be written as:

$$\begin{aligned} \Delta L_{AB}^j &= \Delta \rho_{AB}^j + c\Delta \tau_{AB} + \Delta Z_{AB}^j - \Delta I_{AB}^j + \Delta B_{AB}^j \\ \Delta L_{AB}^k &= \Delta \rho_{AB}^k + c\Delta \tau_{AB} + \Delta Z_{AB}^k - \Delta I_{AB}^k + \Delta B_{AB}^k \end{aligned} \tag{4.29}$$

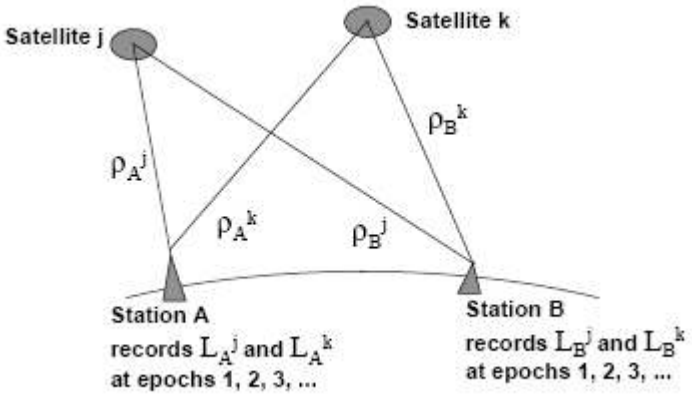

Figure 4.4. Double differencing geometry

And the double difference phase is defined as the difference between equations (4.29):

$$\begin{aligned}\nabla\Delta L_{AB}^{jk} &= \Delta L_{AB}^{j} - L_{AB}^{k} \\ &= \left(\Delta\rho_{AB}^{j} + c\Delta\tau_{AB} + \Delta Z_{AB}^{j} - \Delta I_{AB}^{j} + \Delta B_{AB}^{j}\right) \\ &\quad -\left(\Delta\rho_{AB}^{k} + c\Delta\tau_{AB} + \Delta Z_{AB}^{k} - \Delta I_{AB}^{k} + \Delta B_{AB}^{k}\right) \\ &= \left(\Delta\rho_{AB}^{j} - \Delta\rho_{AB}^{k}\right) + \left(c\Delta\tau_{AB} - c\Delta\tau_{AB}\right) \\ &\quad + \left(\Delta Z_{AB}^{j} - \Delta Z_{AB}^{k}\right) - \left(\Delta I_{AB}^{j} - \Delta I_{AB}^{k}\right) - \left(\Delta B_{AB}^{j} - \Delta B_{AB}^{k}\right) \\ &= \nabla\Delta\rho_{AB}^{jk} + \nabla\Delta Z_{AB}^{jk} + \nabla\Delta I_{AB}^{jk} + \nabla\Delta B_{AB}^{jk}\end{aligned} \tag{4.30}$$

Double differences can be linearly dependent. Thus, double differenced observations that involve a common receiver and common satellite are statistically dependent. For example, at a given epoch, double differences L_{AB}^{21}, L_{AB}^{23} and L_{AB}^{24} are correlated due to the single differenced data in common, L_{AB}^{2}. Any measurement error in this single difference will contribute exactly the same error to each of the double differences. This situation where data are correlated, the weighted least squares is appropriate. Constructing of weight matrix **W**, can be generally called the stochastic model which describes the statistical nature of the data (Blewitt, 1997). The weight matrix is inverse of covariance matrix.

$$\mathbf{W} = \mathbf{C}_{\Delta\nabla}^{-1} \tag{4.31}$$

By using the law of propagation of errors, the covariance of double differenced data can be written as (where **D** matrix is the matrix which transform a column vector of recorded data into column vector of double differenced data);

$$\mathbf{C}_{\Delta\nabla} = \mathbf{DCD}^T \tag{4.32}$$

Finally the double differenced data weight matrix can be written as;

$$\mathbf{W} = \left(\mathbf{DCD}^T\right)^{-1} \tag{4.32}$$

As mentioned above the computed covariance matrix of estimated parameters for weighted least squares were $\mathbf{C}_x = (\mathbf{A}^T\mathbf{WA})^{-1}$, so full expression for the computed covariance matrix substituting for the double differenced data weight matrix **W;**

$$\mathbf{C}_x = (\mathbf{A}^T(\mathbf{DCD}^T)\mathbf{A})^{-1} \tag{4.33}$$

4.1.2 Baseline Processing

Processing GPS data has several steps, including the basic of the theory which had already stated above, preparing data, processing procedure and evaluating the outputs. The fundamental unit of a GPS solution is the single baseline solution. Moreover, most GPS data processing software accept only simultaneous phase data collected by two GPS receivers as mentioned above. That is why the modeling of observables is a necessary for GPS phase data reduction, involves two stations defining a baseline. Estimating clock parameters needs collecting data from several sites to several satellites and processing them together.

Baseline solution using phase data has some main steps which can be separated into three parts. Setting up the necessary data for processing is the first step of baseline solution which involves preparation of data, selection of parameters and selection of options. Preparation includes the deciding apriori coordinates, ephemeris file to be used, baselines to be processed, antenna height, etc. Parameter selection depends on the baseline to be processed, the ambiguity model used in software, differencing scheme adopted, and etc. Selection of the options are related with the apriori standard deviation of parameters and observations, criteria for data rejection, whether correlations are to be considered, elevation cutoff, satellites to be excluded from solution and differencing strategy to be used.

The processing step of baseline solution using phase data has at least three steps. Single Difference Solution which provides a good apriori base, Double Difference solution Ambiguity fixed (where the ambiguity parameter values fixed to integer values) and Double Difference solution Ambiguity float (where the ambiguity parameters are floating numbers).

Finally the last step is the output stage which provides the coordinate files in Cartesian and geodetic values in WGS84 datum for ground mark and antenna centers,

estimated standard deviation and covariance matrix of parameters and indicators of quality of the solution.

4.2 GPS Processing Software-High Precision Software

There are several processing software packages, developed since beginning of 1980s. These software packages are capable of acquiring high precision geodetic estimates over long baselines and generally developed by universities and governmental research laboratories.

There are some typical features of these software packages such as, orbit integration with appropriate force models, accurate model with celestial and terrestrial reference systems, reliable data editing (cycle-slips etc.), estimation of all coordinates, orbits tropospheric bias, receiver clock bias, polar motion and Earth spin rate, ambiguity resolution algorithms applicable to long baselines, estimation of reference frame transformation parameters and kinematic modeling of station positions to account for plate tectonics and co-seismic displacements (Blewitt, 1997).

There are three main widely used high-precision software packages have been developed by researchers all around the world and are commonly referenced in the scientific literature:

BERNESE software developed by the Astronomical Institute, University of Berne in Switzerland. GIPSY software developed by the Jet Propulsion Laboratory, California Institute of Technology in USA. GAMIT/GLOBK software developed by the Massachusetts Institute of Technology in USA.

4.2.1. GAMIT/GLOBK

GAMIT and GLOBK are programs for analyzing GPS measurements primarily to study crustal deformation. Software is available on the internet by applying to the MIT in for non-commercial use. GAMIT is collection of programs used for the analysis of GPS data. It uses the GPS broadcast carrier phase and pseudorange observables to estimate 3D relative positions of ground stations and satellite orbits, atmospheric zenith delays, and earth orientation parameters. The software is designed to run under any UNIX operating system.

GLOBK is a Kalman filter whose primary purpose is to combine various geodetic solutions such as GPS, VLBI, and SLR experiments. It accepts as data or "quasi-observations" the estimates and covariance matrices for station coordinates, earth-orientation parameters, orbital parameters, and source positions generated from the analysis of the primary observations. Generally the outputs of the various processing software are available to use as input data to GLOBK in order to combine geodetic solutions.

4.2.2 Steps of Processing in GAMIT

The main GAMIT modules requires seven types of input parameters, raw phase and pseudorange data in the form of ASCII X-Files one for each station within each session, station coordinates in the form of L-File (Figure 4.5.), satellite list and scenario which is session.info (Figure 4.6.), receiver and antenna information for each site which is in station.info (Figure 4.7.), initial conditions for satellites orbit in a G-File (or tabular ephemeris T-File), satellite and station clock values (I-,J-, and K-Files), and control files for the analysis (sestbl. and sittbl).

The L-File is station coordinate file that includes the list of best available coordinates of the sites of the experiment such as;

```
* nafd_plate_scec.apr :  itrf00_noam + updates from vel_020123a
* North American stations for stabilization
*
 GOLD_GPS  -2353614.1450  -4641385.3890   3676976.4750  -0.00216  0.00649  0.00457  1997.0000
 MOJ1_GPS  -2356424.5422  -4646613.6634   3668462.2248  -0.00216  0.00649  0.00457  1991.0600
 MOJ1_GLA  -2356424.5553  -4646613.5858   3668462.2288  -0.00216  0.00649  0.00457  1998.9610
 GOLD_GHT  -2353614.1949  -4641385.3488   3676976.4648  -0.00216  0.00649  0.00457  2000.6690
```

Figure 4.5. An example of L-File

It is important to select good apriori coordinates for processing. The first consideration is to generate pre-fit residuals sufficient for autocleaning to perform robust editing of the data.

Session.info file is the session information or the processing scenario file. This file contains the start time, sampling interval (i.e. 10 seconds), number of observations, and PRN number of satellites to be used in generating X-Files such as;

```
* session.info: free format, non-blank first column is comment
*Year Day Sess#  Interval  #Epochs  Start hr/min  Satellites
 1986 278  1          30      900       14 04       3   6   9  11  12  13
 1986 350  1          30      900        8 10       3   6   9  11  12  13
 1986 351  1          30      900        8 06       3   6   9  11  12  13
 1987 144  1         120      225       22 52       3   6   8   9  11  12 13
```

Figure 4.6. An example of session.info file

Station.info file contains the station information, including all the receiver and antenna information specific to a particular site occupation. This file has to be created manually and is an input file for GAMIT.

```
# New-style station.info written from old using conv_stnfo by rwk             on 2003-01-13  10:23
*
*SITE  Station Name      Session Start      Session Stop       Ant Ht   HtCod  RcvCod  SwVer  AntCod
#  Global stations
 2353  Wairakei          1990 334  0  0  0  1991 332  0  0  0   1.4116  DHARP  TRMSST   4.10  TRMSST
 2353  Wairakei          1991 332  0  0  0  9999 999  0  0  0   1.4130  DHARP  TRMSST   4.53  TRMSST
 AIS2  Annette Island 2  1996  19  0  0  0  1996 325  0  0  0   0.0000  DHARP  ASHZ12   8.04  ATGE33
 AIS2  Annette Island 2  1996 325  0  0  0  1999 173  0  0  0   0.0000  DHARP  ASHZ12   9.40  ATGE33
 AIS2  Annette Island 2  1999 173  0  0  0  9999 999  0  0  0   0.0000  DHARP  ASHZ12   9.50  ATGE33
 ZWEN  Astronomical Obs  2000 265  0  0  0  9999 999  0  0  0   0.0460  DHARP  AO800A   3.30  TRBROG
#  Regional occupations
 BLHL  Black Hill 1881   1994  66 18 30  0  1994  67  4 30  0   1.3250  SLBGP  TRMSSE   5.71  TRMSST
```

Figure 4.7. An example of station.info file

Sittbl is the input control file for FIXDRV, and specifies the clock and atmospheric model to be used for each site, and apriori coordinate constraints. Sestbl. is an input control file for FIXDRV, specifying the type of analysis the a priori measurement errors and constraints.

The G-File contains initial conditions and nongravitational force parameters for each GPS satellite at particular UTC epoch. The G-File initial conditions serve as starting points for a numerical of satellite orbits and the generation of tabular ephemeris file (T-File) for all satellites in a session. The most accurate and and reliable method of obtaining a starting T-File is first to download precise ephemeris orbits SP3 file from SOPAC Data archive (http://sopac.ucsd.edu/dataArchive/).

Pre-processing begins by creating links within the day directory (experiment directory) to the data files and tables necessary to set up the batch processing. For this purpose creating links to GAMIT global files geodetic datums (gdetic.dat) which is table of parameters of geodetic datums specified by the standard ellipsoid parameters, lunar and solar ephemerides (luntab. and soltab.), nutations (nuttab.), Earth rotation (ut1. and pole.), ocean tides (stations.oct and grid.oct), leap seconds (leap.sec), and spacecraft, receiver, and antenna characteristics (svnav.dat, antmod.dat, rcvant.dat) has to be performed.

After the preparation of the data in RINEX observation and navigation files and creating station.info and session.info files, the program MAKEXP, was executed to generate most of the additional files, which are needed to complete preprocessing. MAKEXP determines the stations to be included in a session from RINEX or X-files. From a scenario file, session.info will be used data to determine the start and stop times of the session and the satellites used in the session. After MAKEXP, the orbital information input is created. Orbital information should be in the form of a tabular ephemeris (T-) file, which contains the positions of the satellites at 15-minute intervals throughout the observation span, or a G-file of initial conditions and can be downloaded from SOPAC data archive. After execution of a 'ephemeris fit' script, the G-file of orbital initial conditions and T-file of tabular ephemeris are obtained. In order to account properly for clock effects in the phase observations, additional information has to be supplied about the behavior of the satellite and station clocks. It was done using the MAKEJ function which is using the RINEX navigation file to make the satellite clock file. In the next processing step, the J-file is used to generate a K-file of station clock offsets.

The next stage of the processing of the session data is to make a station clock offset file, K-file and observation X-files for each station in the session. This is done with the MAKEX program. Its as inputs are the scenario file (session.info), station information file (station.info), satellite clock (J-) file, broadcast ephemeris (RINEX navigation) file, station coordinates (L-) file, and raw data files, and creates X- and K-files. The X-files are the key organizational structure because all X-files for given session are written with the same start and stop times, selection of the satellites, and sampling interval. This imposed rigidity has certain advantages. The primary one is the process of creating the X-files acts as a filter, catching most of the problems with missing or invalid data, mismatched time tags, and poorly behaved receiver clocks that would cause greater loss of time if discovered later. K–file obtained after MAKEX processing contains the values of receiver clock offset during observation span, from pseudorange. The K-file includes the pseudoranges to the particular satellites in units of seconds at the time given, the offset of the satellite clock computed from the transmitted clock corrections and correction of receiver clock.

Finally the FIXDRV program, executes the GAMIT programs MODEL (computes the theoretical values of the observations and partial derivatives of these observations with respect to the parameters to be estimated and writes them to an output C-File for editing and estimating), AUTCLN (performs automatic editing for cycle-slips and outliers in the phase observation), CFMRG (writes a file, (M-File) defining the way observations are to be combined), and SOLVE (performs least squares analysis, writing the output to a Q-File and the adjustments and covariance matrix to an H-File for combination of other sessions and experiments using GLOBK).

In practice the primary indicator in evaluating the solutions is the "normalized rms" (nrms) of the solution; the square root of chi-square per degree of freedom. Generally with the default weighting scheme, a good solution produces a nrms of about 0.25. Any nrms value larger than 0.5 means that there are cycle slips that have not been removed, associated with extra bias parameters, or bad coordinate of the fixed stations.

GLOBK is a Kalman filter which primary purpose is to combine solutions from the processing of primary data from space-geodetic or terrestrial observations. It accepts as data - the estimates and associated covariance matrices for station coordinates, earth rotation parameters, orbital parameters, and source positions generated from analyses of the primary observations. These primary solutions should be performed with loose a priori uncertainties assigned to the global parameters, so that constraints can be applied uniformly in the combined solution (GLOBK reference Manual). GLOBK is used to combine individual sessions of observations in order to estimate station coordinates that is averaged multi-day experiment. Another application that GLOBK used is combination of experiment averaged estimates of station coordinates obtained from several years of observations to estimate station velocities. Finally, for the combination of individual sessions or experiments with station coordinates treated as stochastic, thus generating coordinate repeatability for assessment of measurement precision over days or years.

GLOBK established on three main programs which are *glred*, *globk* and *glorg*. *Glorg*, as an origin fixing program allows the reference frame of solution to be specified after all data have been combined by *globk*. *Globk* is a Kalman filter for combining several solutions from primary single session observations. *Glred* is similar to *globk* but it treats the H-files from each day independently, providing a method for generating coordinate repeatability which is more efficient than a rigorous Kalman back solution performed by *globk*. It is simply a front-end program to drive globk, in other words, it allows many runs of globk using a single command and produces for each session independent solution, neglecting the correlations between different sessions.

4.2.3 General Interpretation

GAMIT/GLOBK is a powerful tool for GPS processing. Nowadays there are a lot of new tools are developing for the outputs of GAMIT process. One of the most popular one is the GAMIT/GLOBK Matlab Tools developed by Thomas Herring and Simon McClusky from MIT. These tools are provided as a means to help users understand the quality of the results being obtained from GLOBK analyses of GPS data. According to the developers, the primary aim is improve the quality and understanding of the results from large GPS analysis projects. There are much more tools for the researchers which not going to be mentioned here.

Table 4.1. Program input and output files

INPUT	OUTPUT	
makexp	- RINEX (or X-) files - station.info - session.info	- D-file - session.info (optional) - Input batch files for *makex*, *makej*, *bctot*
makej	- RINEX nav file - C-file (optional--See 4.6)	- J-file (satellite clock file)
makex	- raw observations (RINEX or FICA) - station.info (rcvr, ant, firware, HI) - session.info (scenario file) - RINEX nav file - J-file (satellite clock file) - L-file (coordinates of stations)	- K-file (receiver clock) - X-file (input observations)
arc	- arc.bat (batch input file) - G-file (orbital initial conditions)	- arcout.ddd (output print file) - T-file (tabular ephemeris for all sat. ses.)
fixdrv	- D-file (list of X-, J-, L-, T-files) - sestbl. (session control) - .sittbl. (site control) - T, J, L, X (or C) input	- B-file (bexpy.bat : primary batch file) - B-file (bexpy.nnn : secondary batch files) - I-file (rcvr clock polynomials)
model	- L-file (site coordinates) - station.info (ant heights) - X-file - I, J, T-files - antmod.dat (PCV models) - RINEX met file - otl.list/grid, atml.list/grid	- C-file (residuals and partials) - P-file (documentation of models)
autcln	- C-file	- C-file (cleaned)
cfmrg	- C-file	- M-file (points to the C-files)
solve	- C-file - M-file	- Q-file - G-file - H-file - L-file
makek	- RINEX nav file - J-file - L-file - X-file	- K-file
ngstot	- SP3-file	- G-file - T-file
bctot	- RINEX nav file	- G-file - T-file

5. FUTURE ASPECTS AND CONCLUSIONS

Thesis focused on the idea of dealing with a crustal deformation monitoring project by using geodetic techniques. Moreover, this study tried to form interactions between geosciences and geodesy in terms of deformation monitoring projects. Geologic and geophysical evidences and researches are incorporated in order to form these interactions and detailed tectonics of the region is introduced. The importance of the region is underlined by adding the tectonics of the region by introducing its relationships with adjacent tectonic phenomenon. In other words, the study explained the tectonics of the eastern Mediterranean and Aegean Region in general and the tectonics of Izmir and its surrounding area more detail. Important faults are underlined from a recent study performed by General Directorate of Mineral Research and Exploration in 2005. Some projects that have geodetic components were also investigated (McClusky *et al*., 2000, Aktug and Kilicoglu, 2006, Reilenger *et al.*, 2002, Reilenger *et al*., 2006) to focus on the movements of Anatolia and western Turkey.

According to the study of McClusky *et al.*, (2000), the high rate of velocity vectors especially in the Aegean Region can be easily seen in Figure 5.1. Moreover, Reilenger *et al.*, (2006), mentioned the high rate of movement of western Anatolia according to the Anatolian plate. Another recent study (Aktug and Kilicoglu, 2006) that covers an area between latitudes 37^0 45’ and 39^0 00’, and longitudes 26^0 00’ and 28^0 00’ mention the high rate of velocities especially near Tuzla fault. the velocities from two different studies can be seen in the Figure 5.2. where the black arrows indicates the residual velocities obtained by differentiating ITRF2000 and Eurasia plate velocities by using the following formula. On the other hand, red colored velocities indicate the Eurasia fixed velocity vectors.

$$v_r = \hat{v}_{ITRF2000} - \hat{v}_{PLATE} \tag{5.1}$$

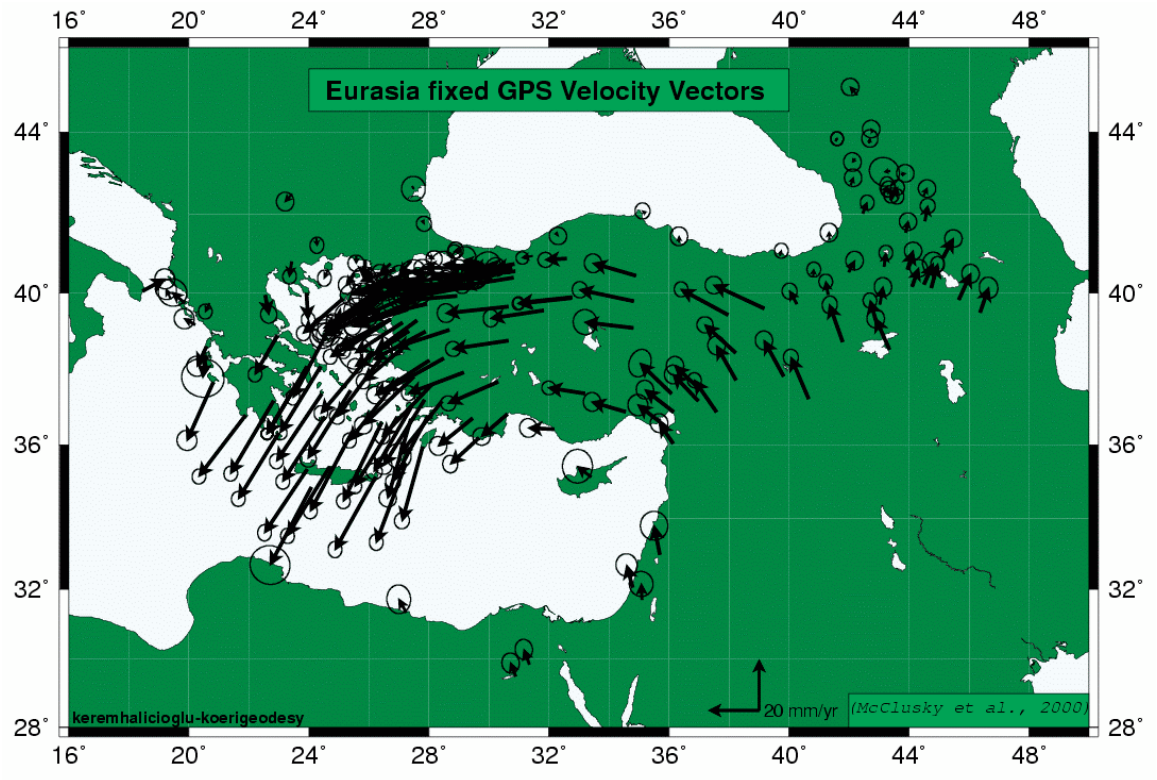

Figure 5.1. Eurasia fixed velocity vectors (McClusky *et al.*, 2000)

In order to contribute these projects by performing large scale fault based deformation monitoring study, Tuzla fault and its vicinity was selected considering its high seismic risk underlined in previous chapters. Therefore, a reconnaissance planned after the literature research in order to investigate the field and collect necessary information from local resources. Thus, the reconnaissance to the region performed, the information collected evaluated and they were analyzed within this study. Moreover, first order network design problems are quoted to create a harmony between microgeodetic networks. Network stations are selected from a large set of control points according to the suggestions mentioned in several studies. Finally, the theoretical background of GPS processing is reviewed and a special processing software GAMIT/GLOBK is introduced. Some additional information is underlined about the software which is studied during this study by the author. These whole processes produced a microgeodetic network that is selected from a huge set of information. Designed network introduced in Chapter 3.

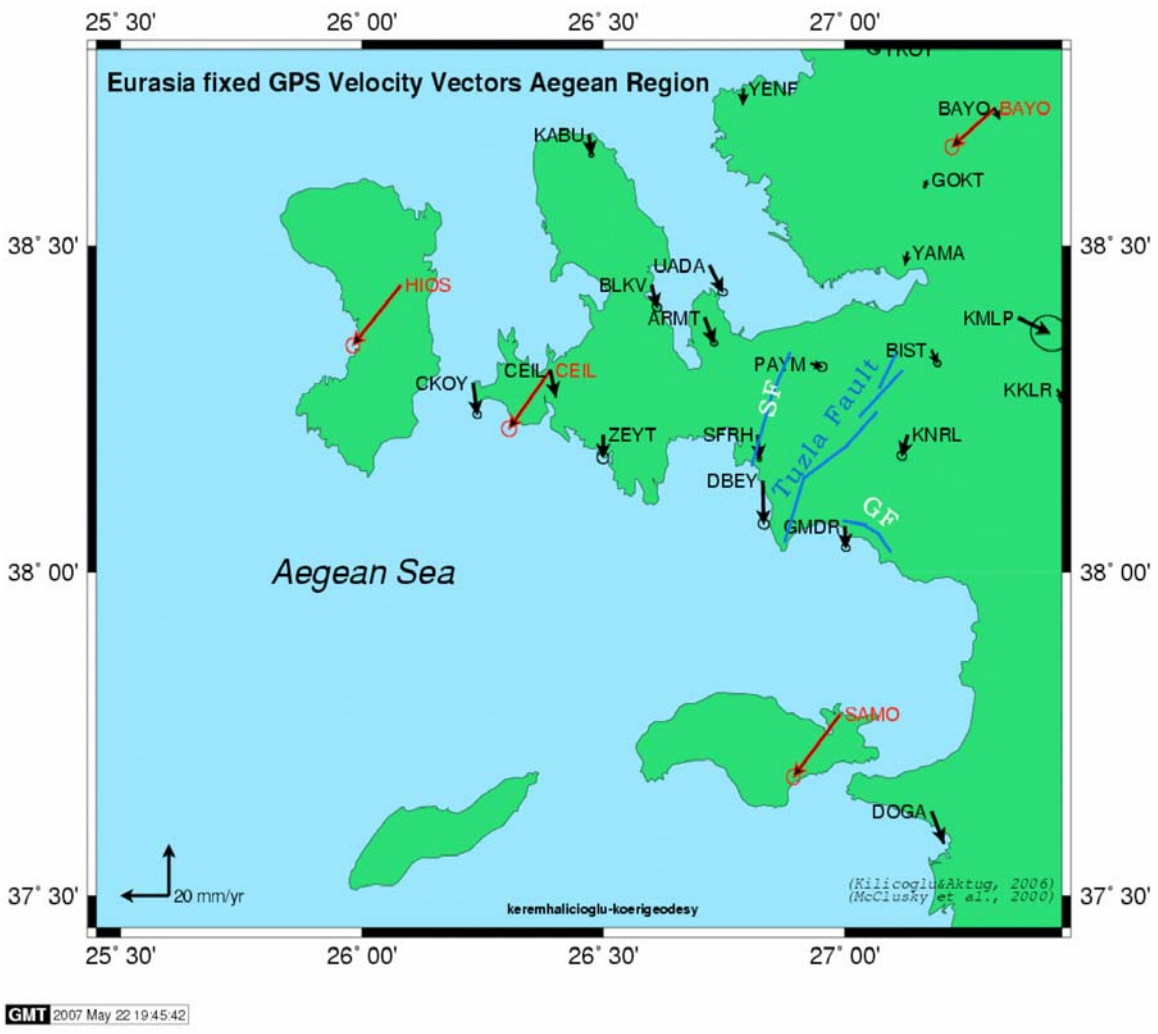

Figure 5.2. Eurasia fixed velocities from two different studies (Aktug and Kilicoglu, 2006, McClusky *et al.*, 2000), blue lines indicate faults (SF: Seferihisar Fault, GF: Gümüldür Fault).

The network has an open end for future studies. In other words, there is a possibility of an extension for the network in order to monitor some additional faults. Tuzla fault, as mentioned in Chapter 2, exists in the center of the region and is very near to the big metropolitan city, Izmir. Thus the origin of the study is selected near this fault. Some researchers also mention the high seismic risk of the region including Tuzla fault (Zhu *et al.*, 2006a, Ocakoglu *et al.*, 2005a). On the other hand, it is certain that the area should be monitored by a larger and dense network with continuously operating GPS stations. However, this is not the economical case of deformation monitoring for present projects.

For further studies, campaign based GPS observations are planned beginning from the current network designed in this study and will extend to the west to the Karaburun Peninsula, and to the east to the eastern Aegean region.

According to the results achieved from personal contact to Esen Arpat, there is a great seismic risk through the transform faults to the east near Pamukkale-Denizli. However, in this study, because of the topography related effects such as high mountains and the small rate vertical deformation make it nearly impossible to study with GPS or precise leveling techniques. For the reasons mentioned above, the network established to the area that is covering the Tuzla fault.

In conclusion, this study, prepare a schedule for deformation monitoring studies using geodetic techniques including network design and optimization. The next step of this study will be three GPS campaigns on the designed network in two periods. In addition to GPS technique, conventional geodetic techniques such as precise leveling technique would be a choice for normal faults where small vertical deformations need to be determined. Further studies will be built on the information and techniques introduced in this study. It is certain that geodetic techniques are capable to determine small quantities of movements which is quite valuable information for earth sciences.

Finally, a researcher has a mission of explaining and publishing his/her studies not only to the scientific field also his own people. Natural hazards like earthquakes were always related to the supernatural phenomena such as religion or mythology for thousands of years. In ancient Greek, for instance, earthquakes were thought to be a punishment of the god Poseidon, god of seas and earthquakes. People used to belive that the god Poseidon rode his horses along the agean sea and people thought that the sound during the eathquake was the sound of the Poseidon’s running horses. They though that it was the anger of the god. Actually, that belief is not so different in many regions all around the world. People still relate natural hazards with metaphysical phenomena even in Anatolia. That’s why the researchers and the scientists of this field, should take their responsibility seriously for

sharing the scientific results of their researches with the common people. Only by this way maybe, the mentality of believing in the superstitious reasons of earthquakes can change with the help of the scientific results presented to them.

REFERENCES

Aktug, B., and Kilicoglu A., "Recent Crustal Deformation of Izmir, Western Anatolia and Surrounding Regions as Deduced from Repeated GPS Measurements and Strain Field", *Journal of Geodynamics* ,Vol. 41, No. 5, pp.471-484, 2006.

Arpat, E., Bingol, E., "Discussions on the Evolution of the Aegean Region Grabens", *General Directorate of Mineral Research and Exploration Institute*, 1969.

Ayan, T., *Optimization of Geodetic Networks*, Associate Professorship Thesis, Istanbul Technical University, Istanbul, Turkey, 1981.

Bagci, G., "Seismic Risk of Izmir and its Surrounding Region", *Proceedings of International Symposia on Seismicity of Western Anatolia*, Izmir, 24-27 May 2000.

Barka, A., Reilinger, R. ve Emre, Ö., "Transform/Ridge/Transform Triple Junction in Western Anatolia", *Proceedings of International Symposia on Seismicity of Western Anatolia*, 24-27 May, 2000.

Barka, A., Reilinger, R., "Active tectonics of the Eastern Mediterranean region: deduced from GPS, neotectonic and seismicity data", *Annali Di Geofisica*, Vol.40, pp. 587–610, 1997.

Blewitt, G., "Basics of the GPS Technique: Observation Equations", *Geodetic Applications of GPS*, Swedish Land Survey, 1997.

Blewitt, G., "Geodetic Network Optimization for Geophysical Parameters", *Geophysical Research Letters*, Vol. 27, No. 22, pp. 2615-3618, November 15, 2000.

Emre, O., Barka, A., “Active Faults between Gediz Graben and Aegean Sea (Izmir Region)”, *Proceedings of International Symposia on Seismicity of Western Anatolia*, 24-27 May, 2000.

Emre, O., Ozalp, S., Dogaz, A., Ozaksoy, V., Yildirim, C., Goktas, F., “The Report on Faults of Izmir and its Vicinity and their Earthquake Potentials”, *General Directorate of Mineral Research and Exploration Report No. 10754*, 2005.

Ergun, M., Oral, E. Z., “General tectonic elements of the Eastern Mediterranean and implications” *Proceedings of International Symposia on Seismicity of Western Anatolia*, Izmir, 24-27 May, 2000.

Genc, C., Altunkaynak, S., Karacik, Z., Yazman, M., Yilmaz, Y., “The Cubuklu Graben, South of Izmir: Tectonic Significance in the Neogene Geological Evolution of the Western Anatolia.”, *Geodinamica Acta*, Vol. 14, No. 1/3, pp. 45-55 2001.

Gerasimenko, M. D., Shestakov, N. V., and Kato, T., “On Optimal Geodetic Network Design for Fault-Mechanics Studies” *Earth Planets Space,* Vol. 52, pp. 985-987, 2000.

Inci, U., Sozbilir, H., Sümer, O., Erkul, F., “The Reasons of Urla-Balikesir Earthquakes”, *Journal of Cumhuriyet, Science and Technique*, 21 June 2003.

Jackson, J., Haines, J. & Holt, W., “A comparison of satellite laser ranging and Seismicity Data in the Aegean Region”, *Geophysical Research Letters,* Vol. 21, pp. 2849-2852, 1994.

Keller, A. E., Pinter N., “Active Tectonics: Earthquakes, Uplift, and Landscape”, *Upper Saddle River, N.J.*, Prentice Hall, 1996.

Kocyigit, A., “Seismicity of Southwestern Turkey”, *Proceedings of International Symposia on Seismicity of Western Anatolia*, Izmir, 24-27 May, 2000.

Kreemer, C., and Chamot-Rooke, N., "Contemporary Kinematics of the Southern Aegean and the Mediterranean Ridge", *Geophysical Journal International* Vol. 157, pp. 1377-1392, 2004.

McCklusky, S., Balassanian, S., Barka, A., Demir, C., Ergintav, S., Georgiev I., Gurkan, O., Hamburger, M., Hurst, K., Kahle, H., kastens, K., Kekelidze, G., King, B., Kotzev, V., Lenk, O., Mahmoud, S., Mishin, A., Nadaria, M., Ouzoun,s, A., Paradissis, D., Peter, Y., Prilepin, M., Reilinger, R., Sanli, I., Seeger, H., Tealeb, A., Toksoz, M. N., Veis, G., "Global Positioning System Constraints On Plate Kinematics And Dynamics In The Eastern Mediterranean And Caucasus", *Journal of Geophysical Research*, Vol. 105, No. B3, pp. 5695-5719, March 10, 2000.

McKenzie, D. P., "Active tectonics of the Mediterranean Region", *Geophysical Journal of Research"*, Vol. 30, pp. 109-185, 1972.

Mercier, J., Sorel, D., Vergely, P., Simeakis, K., "Extensional tectonic regimes in the Aegean basins during the Cenozoic", *Basin Research*, Vol. 2, pp. 49-71, 1989.

Monroe J. S., *Physical Geology*, Thomson Learning, 1996.

Müller, S., Kahle, H. G., and Barka, A., "Plate Tectonics situation in the Anatolian-Aegean Region", *Active Tectonics of Northwestern Anatolia- the Marmara Poly-project*, 1997.

Nur, A., Cline, E. H., "Poseidon's Horses: Plate Tectonics and Earthquake Storms in the Late Bronze Age Aegean and Eastern Mediterranean", *Journal of Archaeological Science*, Vol. 27, pp. 43–63, 2000.

Ocakoglu, N., Demirbas, E., Kuscu, I., "Neotectonic structures in Izmir Gulf and Surrounding Regions: Evidences of Strike-Slip Faulting with Compression in the Aegean Extensional Regime", *Marine Geology*, Vol. 219, pp. 155–171, 2005a.

Ocakoglu, N., Demirbas, E., Kuscu, I., "The Submarine Active Faults and the Seismicity of the Gulf of Izmir and Surrounding Area" *Journal of the Earth Sciences Application and Research Centre of Hacettepe University*, Vol. 27(1), pp. 23-40, 2005b.

Ozcep, F., "Has Central Anatolia A Micro-Plate Behavior Within Turkish Plate? A Paleomagnetic Discussion" *International Conference on Earth Sciences and Electronics (ICESE 2002)*, 2002.

Ozener, H., *Monitoring Regional Horizontal Crustal Movements by Individual Microgeodetic Networks Established Along Boundaries,* Ph.D. Thesis, Bogazici University, Istanbul, Turkey, February, 2000.

Ozmen, B., Nurlu, M., Güler, H., *Investigation of Earthquake Zones with Geographic Information Systems*, The Ministry of Public Works and Settlement General Directorate of disaster Affairs, 1997.

Papazachos, C. B., "Seismological and GPS evidence for the Aegean Anatolia Interaction", *Geophysical Research Letters*, Vol. 17, pp. 2653-2656, 1999.

Piper, J., Gursoy, H., and Tatar, O., "Palaemagnetic analysis of Neotectonic Crustal Deformation in Turkey", *Proceeding of Symposia on Seismotectonics of the North-Western Anatolia-Aegean and Recent Turkish Earthquakes,* 8 May, 2001.

Reilinger, R., McClusky, S., Vernant, P., Lawrence,S., Ergintav, S., Cakmak, R., Ozener, H., Kadirov, F., Guliev, I., Stepanyan, R., Nadariya, M., Hahubia, G., Mahmoud, S., Sakr, K., ArRajehi, A., Paradissis, D., Al-Aydrus, A. Prilepin, M., Guseva, T., Evren, E., Dmitrotsa, A., Filikov, S. V., Gomez, F., Al-Ghazzi, R., Karam, G., "GPS Constraints on Continental Deformation in the Africa-Arabia-Eurasia Continental Collision Zone and implications for the Dynamics of Plate Interactions", *Journal of Geophysical Research,*Vol.111, B05411, 2006.

Reilinger, R.E., Ergintav, S., Burgmann, R., McClusky, S., Lenk, O., Barka, A., Gurkan, O., Hearn, L., Feigl, K. L., Cakmak, R., Aktug, B., Ozener, H., Toksoz, M. N., "Coseismic and Postseismic Fault Slip for the 17 August 1999 M=7.5 Izmit, Turkey Earthquake", *Science,* Vol. 289, pp. 1519, 2000.

Saroglu, F., Emre, O., and Kuscu, I., "Turkish Active Faults Map" *General Directorate of Mineral Research and Exploration*, Ankara, 1992.

Segall, P., Davis, J. L., "GPS Applications for Geodynamics and Earthquake Studies", *Annual Review Earth Planet Sci.*, Vol. 25:301-36, 1997.

Shestakov, N.V., Waithaka, H.E., Kasahara, M., Gerasimenko, M.D., "Two Examples Of Optimal Design Of Geodynamic GPS Network*", International Associations Of Geodesy Symposia,* Vol. 128, Ed. F.Sanso, 30, June- 11, July, Sappporo, Japan, 2003.

Tan, O., and Taymaz, T., "Seismotectonics of Karaburun Peninsula and Kuadasi Gulf: Source parameters of April 2, 1996 Kuadasi Gulf and April 10, 2003 Seferihisar (Izmir) Earthquakes", *International Workshop on the North Anatolian, East Anatolian and Dead Sea Fault Systems: Recent Progress in Tectonics and Paleoseismology and Field Training Course in Paleoseismology*, *Middle East Technical University*, 2003.

Taskin, G., Uskuplu, S., Saygin, H., Ergintav S., "Optimization of GPS Observation Strategy for Improvement of Tectonic Measurements", *Proceedings of Applied Simulation and Modelling Conference*, Marbella, Spain, 2003.

Taymaz, T., "Active Tectonics of the North and Central Aegean Sea" *Proceeding of Symposia on Seismotectonics of the North-Western Anatolia-Aegean and Recent Turkish Earthquakes*, 8, May, 2001.

Taymaz, T., Jackson, J. A., and Mckenzie, D., "Active Tectonics of the north and Central Aegean Sea", *Geophyical Journal Internationa.*, Vol. 106, pp. 433-732, 1991.

Türkelli, N., Kalafat, D. ve Gündodu, O., "November, 6, 1992 Izmir (Doganbeyli) Earthquake, Field Observations and Focal Mechanism Solutions", *Geophysics (in Turkish)*, 1995.

Türkelli, N., Kalafat, D., Ince, S., "After shocks of November, 6, 1992 Izmir (Doganbeyli) Earthquake", *Bulletin of Earthquake Investigations*, 1992.

Utku, M., "Position of Western Anatolia in Turkey's Seismicity", *Proceedings of International Symposia on Seismicity of Western Anatolia*, 24-27 May, 2000.

Wu, J., Tang, C., and Chen, Y. Q., "First-order Optimization for GPS Crustal Deformation Monitoring" *Proceedings of the 7th South East Asian Surveying Congress*, Hong Kong, China, 3-7 November, 2003.

Yilmaz, Y., "Active tectonics of Aegean Region", *Proceedings of International Symposia on Seismicity of Western Anatolia*, 24-27 May, 2000.

Zhu, L., Akyol, N., Mitchell, B. J., Sozbilir, H., "Seismotectonics of Western Turkey from High Resolution Earthquake Relocations and Moment Tensor Determinations" *Geophysical Research Letters,* Vol. 33, 2006a.

Zhu, L., Mitchell, B. J., Akyol, N., Cemen, I., Kekovali, K., "Crustal Thickness Variations in the Aegean Region and its Implications for the Extension of Continental Crust" *Journal of Geophysical Research*, Vol. 111, 2006b.

Mckenzie, D., "Active Tectonics of Alphine-Himalayan Belt: The Aegean Region and Surrounding Regions", *Geophysical J. R. Ast. Soc.*, Vol. 55, pp. 217-254, 1978.

REFERENCES NOT CITED

Aktug, B., "ITRF velocity Field and a Look at Relative Velocity Frames", *Journal of Map* (in Turkish), 2003.

Altiner, Y., "The Contribution of GPS data to the Detection of the Earth's Crust Deformations Illustrated by GPS Campaigns in the Adria Region", *Geophysical Journal International*, Vol. 145, pp. 550–559, 2001.

Banjeree, P., Satyaprakash, W., "Crustal Configuration across the North-Western Himalaya as Inferred from Gravity and GPS Aided Geoid Undulation Studies", *Journal of the Virtual Explorer*, Vol. 12, pp. 93-106, 2003.

Blewitt, G., "Fundamental ambiguity in the definition of vertical motion", *Cahier du Centre Européen de Géodynamique et de Séismologie*, Vol. 23, pp. 1-4, 2004.

Blewitt, G., and Lavallee, D., "Effect of annual signals on geodetic velocity", *Journal of Geophysical. Research*, Vol. 107 B7, 2002.

Bock, Y., Prawirodirdjo, L., "Detection of Arbitrarily Large Dynamic Ground Motions with a Dense High-Rate GPS Network", *Geophysical Research Letters*, Vol.31, 2004.

Bozkurt, E., "The Evolution of Large Scale Normal Faults", *Seminar on the Aykut Barka Conference*, 2006.

BU KOERI, "Preliminary Report on October, 19-21, 2005 Gulf of Sigacik-Seferihisar (Izmir) Earthqukes", *Technical Report*, 2005.

Campbell, J., Nothnagel, A., "European VLBI for Crustal Dynamics", *Journal of Geodynamics* Vol. 30, pp. 321-326, 2000.

Carminati, E., Doglioni, C., Gelabert, B., Panza, G. F., Raykova, R. B., Roca, E., Sabat, F., Scrocca, D., "Evolution of the Western Mediterranean", *Principles of Phanerozoic Regional Geology*, 2004.

Christova, C., Nikolova, S. B., "Contemporary Plate Tectonics in The Aegean Region by Seismological Studies", *National Conference with international participation, Bulgarian Geophysical Society*, 2006.

Davies, P., and G. Blewitt, "Methodology for global geodetic time series estimation: A new tool for geodynamics", *Journal of Geophysics* Research, Vol. 105, No. B5, pp. 11,083-11,100, 2000.

Emre, T., "Tectonical Evolution of the Gediz graben", *Geological Bulletin of Turkey*, V. 39, No 2, pp. 1-18, August, 1996.

Eshelby, J. D., "Dislocation Theory for Geophysical Applications", *Philosophical Transactions of the Royal Society of London, Series A., Mathematical and Physical Sciences*, Vol.274, No.1239, 1973.

Eyidogan, H., "Tectonics and Earthquake Danger", *Fifth National Conference on Earthquake Engineering*, 26-30 May, 2003.

Gautier, P., Brun, J. P., Moriceau, R., Sokoutis, D., Martino, J., Jolivet, L., "Timing, kinematics and cause of Aegean extension: a scenario Based on a comparison with simple analogue experiments", *Tectonophysics*, Vol. 315, pp. 31-72, 1999.

General Command of Mapping-Turkey, "Turkish National Fundamental GPS Network", *Technical Report*, 2001.

Halicioglu, K., Ozener, H., Unlutepe, A., "Network Design and Optimization for Deformation Monitoring on Tuzla Fault-Izmir and its Vicinity, *International Symposium Modern Technologies", Education and Professional Practice in Geodesy and Related Fields,* 2006.

Hammond, W. C., Thatcher, W., "Northwest Basin and Range Tectonic Deformation Observed with the Global Positioning System,1999–2003", *Journal Of Geophysical Research,* Vol.110,B10405, 2005.

Herring, T. A., King, R. W., McClusky, S. C., "GAMIT Reference Manual GPS Analysis at MIT Release 10.3" *Department of Earth, Atmospheric, and Planetary Sciences Massachussetts Institute of Technology*, 2006.

Herring, T. A., King, R. W., McClusky, S. C., "Introduction to GAMIT/GLOBK Release 10.3*", Department of Earth, Atmospheric, and Planetary Sciences Massachusetts Institute of Technology,* 2006.

Herring, T. A., King, R. W., McClusky, S. C., "Global Kalman filter VLBI and GPS analysis program*" Department of Earth, Atmospheric, and Planetary Sciences Massachusetts Institute of Technology*, 2006.

Karabulut, H., Ozalaybey, S., Taymaz, T., Aktar, M., Selvi, O., Kocaoglu, A., "A Tomographic image of the Shallow Crustal Structure in the Eastern Marmara", *Geophysical Research Letters,* Vol.30, No.24, 2003.

Kiger, M., Russel, J., "This Dynamic Earth", *USGS Publication,* 1996.

Koral, H., Yilmaz, M., "The Çay–Eber Earthquake (Feb. 3, 2002; Mw=6.2), Western Turkey: A Review in Geological Context", *International Conference on Earth Sciences and Electronics,* 2003.

Ozener, H, Garagon Dogru, A, Halicioglu, K, Ergintav, S, Cakmak, R, Arpat, "Deformation Kinematics of Eastern North Anatolian Fault by Geodetic Data", *AGU 2006 Fall Meeting,* San Francisco, California, USA,11-15, December, 2006.

Ozener, H., Turgut, B., Garagon Dogru, A., Halicioglu, K., Avci, O., Yilmaz, O., "GPS Measurements for Investigation of Crustal Deformation and Block Kinematics of the Eastern Part of North Anatolian Fault Zone", *5th International Symposium Turkish-German Joint Geodetic Days,* Technical University, Berlin, Germany, 28-31, March, 2006.

Ozener, H., Turgut, B., Garagon Dogru, A., Halicioglu, K., "Geodetic Determination of Crustal Movements on the NAFZ", *International Symposium Modern Technologies, Education and Professional Practice in Geodesy and Related Fields,* Sofia, Bulgaria, 09-10, November, 2006.

Pratt, D., "Plate Tectonics: A Paradigm under Threat", *Journal of Scientific Exploration,* Vol. 14, No. 3, pp. 307–352, 2000.

Provost, A. S., Chery, J., Hassani, R, "3D Mechanical modeling of the GPS velocity field along the north Anatolian Fault", *Earth Planetary Science Letters,* Vol. 209, pp. 361-377, 2003.

Sandwell, D. T., *Plate Kinematics,* The Solid Earth, C.M.R. Fowler, Cambridge University Press, 1990.

Sezer, I. L., "Earthquake activity and Seismic Risk around Karaburun (Izmir), *Turkey Quaternary Symposium V*, 2005.

Sodoudi, F., Lithospheric *Structure of the Aegean Obtained from P and S receiver Functions*, PhD Thesis, FU Berlin, 2005.

Stangl, G., Bruyninx, C., "Recent Monitoring Of Crustal Movements In The Eastern Mediterranean, the Usage of GPS Measurements", N*ATO Science Series: IV: Earth and Environmental Sciences,* 2006.

Tari, E., Sahin, M.,Barka, A., Reilinger, B.,King, R.W., McClusky, S, Prilepin, M., "Active tectonics of the Black Sea with GPS", *Earth Planets Space*, Vol. 52, pp. 747-751, 2000.

The Ministry of Public Work and Settlement, General Directorate of Disaster Affairs and Earthquake Research Department "Janunary, 29, 2005, Civril (DENIZLI); January, 29, 2005 Seferihisar (IZMIR) and January, 30, 2005 Kas (ANTALYA) Earthquakes", *Press Release*, 2005.

Turcotte, D. L., Schubert, G., *Geodynamics*, Cambridge University Press, 2001.

Unsworth, M., "The Role of Crustal Fluids in Strike-slip Tectonics: New Insights from Magnetotelluric Studies", *Turkish Journal of Earth Sciences (Turkish J. Earth Sci.)*, Vol. 11, pp. 193-20, 2002.

Vanicek, P., *An Online Tutorial in Geodesy*, University of New Brunswick, Academic Press 2001.

Westaway, R., "Kinematics of the Middle East and Eastern Mediterranean Updated", *Turkish Journal of Earth Sciences*, Vol. 12, pp. 5-46, 2003.

Yagmurlu, F., Senturk, M., "Active Tectonics of Southwestern Anatolia", *Turkey Quaternary Symposium V*, 2005.

Yilmazturk, A., Bayrak, Y., Cakir, O., "Crustal Seismicity in and Around Turkey", *Natural Hazards*, Vol. 18, pp. 253–267, 1999.

Zhu, L., Mitchell, B. J., Akyol, N., Cemen, I., Kekovali, K., "Crustal Thickness Variations in the Aegean Region and its Implications for the Extension of Continental Crust", *Journal of Geophysical Research*, Vol.111, 2006.

AUTOBIOGRAPHY

Kerem Halicioglu

Bogazici University, Turkey

Kerem Halicioglu is currently working at Bogazici University as a research assistant in Kandilli Observatory and Earthquake Research Institute, the Department of Geodesy. He got his B.S. degree in Geodesy and Photogrammetry Engineering from Istanbul Technical University in 2003. Since 2002 he has been doing his researches on North Anatolian and East Anatolian Fault Zones. His research interests include Geodesy, Network Design and Optimization, GPS, Crustal Deformation Monitoring, Surveying in Archaeological Sites and excavations, and architectural surveying, modeling and visualization. He has authored or co-authored over 10 scientific papers in various conference proceedings. He is a member of the Turkish Chamber of Surveying Engineers and the American Geophysical Society.